J Mater Sci (2012) 47:553–582
DOI 10.1007/s10853-011-5981-y

ANNIVERSARY REVIEW

Glass–ceramic glazes for ceramic tiles: a review

R. Casasola · J. Ma Rincón · M. Romero

Received: 18 July 2011 / Accepted: 19 September 2011 / Published online: 4 October 2011

Abstract Glass–ceramics are ceramic materials produced through controlled crystallisation (nucleation and crystal growth) of a parent glass. The great variety of compositions and the possibility of developing special microstructures with specific technological properties have allowed glass–ceramic materials to be used in a wide range of applications. One field for which glass–ceramics have been developed over the past two decades is that of glazes for ceramic tiles. Ceramic tiles are the most common building material for floor and wall coverings in Mediterranean countries. Glazed tiles are produced from frits (glasses quenched in water) applied on the surface of green tiles and subjected to a firing process. In the 1990s, there was growing interest in the development of frits that are able to crystallise on firing because of the need for improvement in the mechanical and chemical properties of glazed tiles. This review offers an extensive evaluation of the research carried out on glass–ceramic glazes used for covering and pavement ceramic tile is accomplished. The main crystalline phases (silicates and oxides) developed in glass–ceramic glazes have been considered. In addition, a section focused on glazes with specific functionality (photocatalytic, antibacterial and antifungal activity, or aesthetic superficial effects) is also included.

Introduction

Since their discovery in the early 1950s, glass–ceramic materials have been widely established in: daily life (e.g. kitchen cooktops) [1], industrial applications (e.g. abrasion resistant tiles in industrial pipes), environmental applications (e.g. reuse of wastes) [2–4], biomedical applications (e.g. prostheses for surgical implants) [5–7], architectural applications [8] and in more advanced technological applications (e.g. telescope mirrors, warheads and composite materials) [9–12]. A glass–ceramic is produced from an original glass by a sequential thermal process that involves controlled crystallisation, which consists of the growth of one or more crystalline phases within the vitreous mass. Crystallisation takes place through two steps, nucleation and crystal growth, which can be defined as the thermal and kinetic process under which a structurally amorphous phase (glass) is transformed in a stable solid phase with a regular ordered geometry [13]. This ordering process is a consequence of the energy reduction that occurs when a molten glass is cooled below its temperature. This phenomenon is known by the scientific community through the name "devitrification" because it constitutes a phenomenon opposite to typical glass nature. Nevertheless, what initially was considered an unwanted process in the manufacturing of glass, as the origin of defects, has become an essential mechanism for obtaining glass–ceramic materials with useful technological properties.

The scientific basis of the supercooled liquids was discovered by Tamman in 1903 [13], but it was in the 1960s–1980s when the general theories on nucleation and crystal growth in glasses were well established. Since then, glass–ceramic materials have played a key role in many scientific and technological developments, and there are numerous books [14–17] and review papers [2, 13, 18–24] describing the basis, characteristics, production and properties of these materials. However, to the authors' knowledge, there have been no review papers on glass–ceramic glazes, which

---

R. Casasola · J. M. Rincón · M. Romero (✉)
Group of Glass and Ceramic Materials, Department of Construction, Eduardo Torroja Institute for Construction Sciences—CSIC, 28033 Madrid, Spain
e-mail: mromero@ietcc.csic.es

have been the subject of considerable research in last two decades due to the need to improve the resistance of ceramic tiles in use, for instance, on floors of large commercial areas. In these applications, the traditional glaze has insufficient abrasive resistance and loses its surface characteristics, such as brightness, colour and superficial texture, very easily [25]. Thus, glass–ceramic glazes have been developed to satisfy the requirements of the ceramic tile industry and the demand for coatings with specific properties.

In this article, we present an extensive review of glass–ceramic glazes for covering and pavement ceramic tile. As crystalline phases determine the technological properties and appearance in this type of glaze, the main crystalline phase developed in the glaze has been chosen as the classification criterion.

The glass–ceramic process

The crystallisation of a glass to develop a glass–ceramic material consists of a nucleation stage, in which small seeds or nuclei develop within the glass, followed by heating to a higher temperature (a crystal growth step), which facilitates the enlargement of crystals until they reach the desired size. The nucleation of crystalline phases can take place through two different mechanisms, i.e. *homogeneous nucleation*, when the nuclei arise from their own melt composition in the absence of foreign boundaries, and *heterogeneous nucleation*, when crystalline phases develop from foreign boundaries, such as grain borders or interfaces.

Thermodynamically, the nucleation of a glass below its liquidus temperature begins when an ordered molecular arrangement is possible, resulting in crystalline nuclei (also called seeds or germs). Nucleation involves a decrease in the free energy of the system, and the more favoured the nucleation process is, the higher the energy released in the formation of germs. Kinetically, the rates of nucleation and crystallisation with temperature have two separate maximum intervals (Fig. 1). The nucleation rate depends on both the probability of formation of stable nuclei and the diffusion of atoms necessary for the development of the nucleus. The lower the nucleation temperature is (higher undercooling degree), the greater the energy released in the formation of nuclei and nucleation is favoured to reach a maximum, after which the nucleation rate decreases as developed nuclei produce a strong increase in the melt viscosity, and therefore, the rate of diffusion decreases. The crystal growth stage begins once stable nuclei are formed within the glass, and the crystallisation rate will depend on the ability to transport atoms from the glass network towards the crystalline phase in development. As with nucleation, crystallisation rate also reach a maximum, after which crystallisation is prevented due to the difficulty to dissipate the heat released in the system.

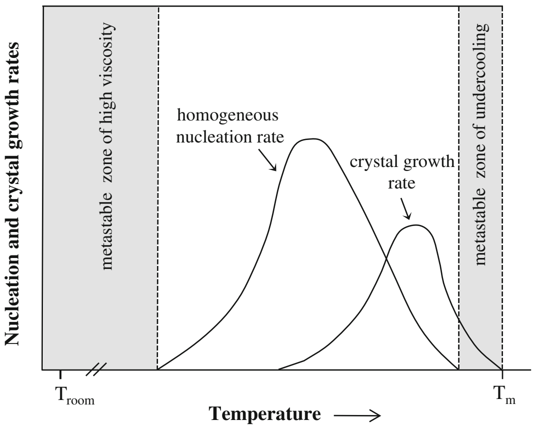

Fig. 1 Variation with temperature of homogeneous nucleation and crystal growth rates in a viscous liquid

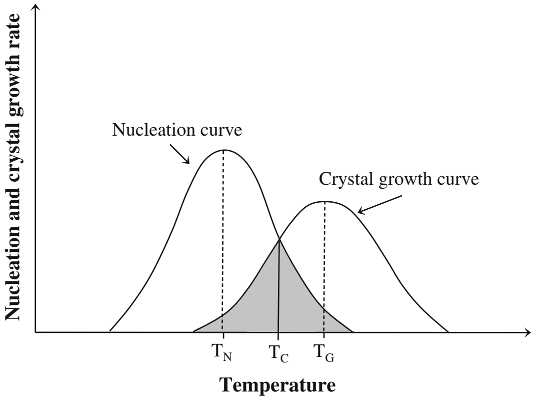

Fig. 2 Relative position of the nucleation and crystal growth curves with temperature

In general, the nucleation and crystal growth curves overlap to some extent, which will determine the most appropriate process for obtaining glass–ceramic from a parent glass. In Fig. 2, the temperatures at which the rates of nucleation and crystal growth are maximised are marked as T_N and T_G, respectively, and T_c is the temperature at which the two curves intersect. The shaded zone indicates the area where the curves of nucleation and crystal growth overlap. The overlap range, T_G–T_N, indicates the optimal temperature range for successfully preparing a glass–ceramic material, i.e. the nucleation stage leads to the formation of a sufficient number of nuclei on which crystals grow, resulting in the fine microstructure desired. If T_N and T_G are far away from T_c, the overlap between the nucleation and crystal growth curves is small and glass–ceramics must be prepared by a two-stage conventional method, in which nucleation and crystal growth occur in separate stages. In contrast, if there is extensive overlap, and both T_N and T_G are close to T_c, glass–ceramics can be produced by a modified (single-stage) process, in which nucleation and crystal growth occur simultaneously.

There are two main routes to the manufacture of glass–ceramic materials (Fig. 3): volume crystallisation from a bulk glass and sinter-crystallisation from a glass powder compact [17]. In volume crystallisation, the nuclei developed in the nucleation stage are homogeneously and randomly distributed throughout the whole volume of the glass. Thus, the stage of crystal growth results in a closely interlocking microstructure with mean crystal size in the region of 1 µm or smaller (50–100 nm). To successfully achieve a glass–ceramic from a bulk glass, controlled crystallisation conditions are required to attain a uniform material, free of defects such as cracks, holes or surface roughness.

Usually, the chemical composition of glasses formulated to develop glass–ceramics by volume crystallisation include nucleating agents, which give rise to discontinuities in the glassy lattice when they are introduced in low percentages in the melt. Habitual nucleating agents are oxides and metallic colloids. Oxides operate by either a valence change mechanism (e.g. metal oxides such as TiO_2, ZrO_2, Cr_2O_3, MnO_2, MoO_3, WO_3 or V_2O_5) or an imbalance charge mechanism (e.g. non-metal oxides such as P_2O_5). Metallic colloids can be introduced in the glass composition as oxides or chlorides and can precipitate metal species by redox or photosensitive reactions (e.g. Cu, Ag, Au, Ru, Rh, Pb, Os, Ir and Pt). Another common nucleating agent in glass–ceramic manufacturing is the F^- ion with an ionic radius similar to that of oxygen that can be introduced into the glass network and lead to the segregation of CaF_2 crystals, which act as nucleating sites. Volume crystallisation can be also produced without the influence of external agents. In this case, a second liquid phase is segregated in the glass matrix and the liquid–liquid immiscibility is responsible for the homogeneous nucleation. However, it has been observed that phase separation in glasses does not always leads to homogeneous nucleation, as the droplet–matrix interfaces may act as heterogeneous nucleation sites [13]. There are three main aspects concerning the relationship between phase separation and nucleation. Volume crystallisation can be attained at earlier stages or delayed by changing the composition of the matrix glass. As a result, surface crystallisation or uncontrolled volume crystallisation can be controlled. A second aspect is that phase separation may form a highly mobile phase that leads to homogeneous crystallisation, while the matrix crystallizes heterogeneously, either in parallel or later. Finally, phase separation processes can lead to interfacial areas that may exhibit preferred crystallisation [18]. Most glass–ceramics are manufactured by controlled nucleation in the volume of the base glass, but there are also glasses in which this procedure is inefficient; volume nucleation cannot be initiated, and controlled crystallisation can be only achieved by surface nucleation. In this case, the most effective method for manufacturing useful glass–ceramics involves the sintering and crystallisation of powdered glass [26, 27]. In this process, glass particles (3–15 µm) must first be compacted by conventional shaping techniques, such as pressing, slip casting or injection moulding. The subsequent thermal treatment to produce a dense glass–ceramic material involves sintering to full density before the crystallisation process is completed.

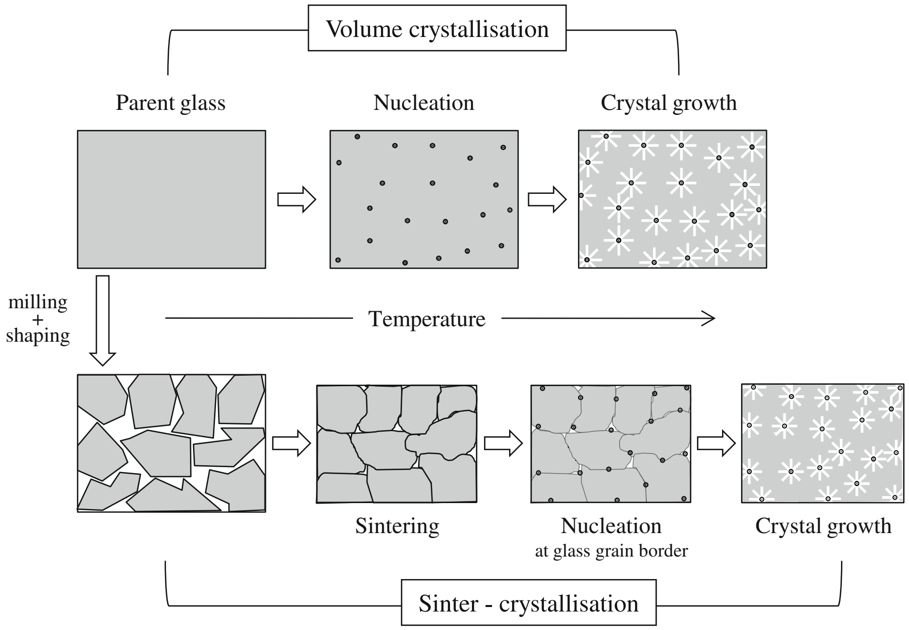

Fig. 3 Evolution of the microstructure from glass to glass–ceramic through volume crystallisation from a bulk glass or sinter-crystallisation from a glass powder compact

The final microstructure of glass–ceramics obtained by both processes (volume or sinter-crystallisation) is similar. The most important advantage of sinter-crystallisation is the ability to use surface imperfections in quenched frits as nucleation sites. Sinter-crystallisation is the method used in the manufacture of glass–ceramic glazes on ceramic tiles, since the only possible way of application of the glaze layer on ceramic supports is as a powder suspension, i. e. as a slip.

Ceramic glazes

A brief history of ceramic glazes

Glazes are stable glassy coatings applied to ceramic earthenware and formerly obtained by cooling oxides or minerals applied and melted on the surfaces of ceramic objects. Originally, glazes were an important innovation for earthenware because, in addition to sealing the porous ceramic surface to avoid evaporation of liquids, they made possible a great variety of decorations. The first glazes were developed around 3500 BC in Eastern Mediterranean countries by potters who tried to imitate the precious blue stone lapis lazuli. For this purpose, small beads were sculpted from steatite ($Mg_3Si_4O_{10}(OH)_2$) and then coated with azurite or malachite powders, natural ores of copper with blue and green colours, respectively. When fired, the coating interacted with the steatite to generate a thin layer of coloured glass. Afterwards, potters started experimenting with different combinations of crushed and ground rock mixed with water to coat the surfaces of pots. They consequently discovered mixtures that completely covered the surfaces of their earthenware with a watertight glassy layer. With the passage of time, potters learned to manufacture glazes in many different colours and textures and even in multiple layers, by using multiple firing cycles at different temperatures [28].

In the second millennium BC, lead glazes were developed in Babylon. Lead acted as a flux, which allowed the glaze to form at lower temperatures. Pigments that lost their colour at higher temperatures could then be used, resulting in brighter and more varied colours. Lead glazes could be applied to the pre-fired ceramic surfaces or over another glaze obtained at a higher temperature, allowing for a wide range of artistic creativity. By the 8th century BC, the Assyrians in Persia discovered another glaze additive: tin oxide. This additive yields a white opaque glaze that could completely cover the brown or reddish colour of clay earthenware [28].

Initially, glazed earthenware was developed because of the need for storage and transportation of liquids and food. Later, due to the aesthetic possibilities afforded by glazes, they started to be used as decorative coating for walls in the form of tiles. One of the earliest and most famous examples of the use of glazed tiles in ancient Mesopotamia is the Ishtar Gate, in the inner wall of Babylon, built under the reign of King Nebuchadnezzar II (in the 6th century BC). Blue, gold-plated and reddish tiles were used to shape both real and mythological animals (Fig. 4).

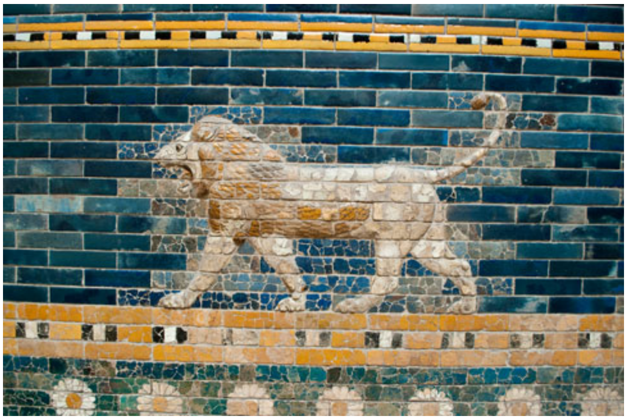

Fig. 4 Lion figure depicted in glazed tile on the Ishtar Gate (Photograph by R. Rincón, taken in the Pergamon Museum, Berlin)

The manufacturing process of glazed ceramic tile

Technical knowledge related to ceramic glazes was kept secret and passed down orally from father to son, so only relatively recent documentation of designs, patterns or procedures are available. Formerly, ceramic tiles were hand-made individually, using the same raw materials that were used for pottery, mostly clay and sand, by pressing and shaping the tile while the clay was still wet and slightly mouldable. The tiles were then sun dried and oven fired. Surprisingly, no major innovations in decorative tile-making occurred until the industrial revolution. In the middle of the 18th century, Richard Prosser invented transfer printing. This process was a new method that could produce glaze designs quickly by using a wooden mould and paper and then transferring the design onto the surface of the tiles. By using this technique, two workers could produce as many tiles in a day (about 1200) as an entire factory of 100 people had been able to produce previously [28].

Another important advance in the manufacturing of ceramic tiles was dust pressing, developed in the middle of the 19th century. The process used previously took a long time because the mixture of clay and water had to be prepared, shaped and dried. Dust pressing is a process that compresses nearly dry clay (5–7% humidity) together with the rest of the tile components. Sufficient pressure could be applied to compact the powder into the desired tile shape. Since the tiles were nearly dry, they could be fired immediately after pressing. This method of shaping tiles is one of the cheapest ways to fabricate ceramic products of regular geometry, and subsequently, the cost of tile production decreased significantly [28].

The firing of ceramic products is one of the most important steps in the manufacturing process because it significantly influences the technological properties of ceramic tiles. Earthenware materials can be fired once, twice or a greater number of times. Unglazed ceramic tiles are fired only once, while glazed tiles can be fired once (*single-firing process*) or twice. In the first firing, the biscuit that will act as a support is fired, and then the glaze is applied and fired in a second thermal cycle (*double-firing process*). In some decorated earthenware materials, a further firing at lower temperatures may be necessary (*third firing*) [28]. Traditionally, the most common method for ceramic tile manufacturing was the double-firing process, with cycles of approximately 40 and 20 h for the first and second firings (biscuit and glaze firing), respectively. Now, the single-firing process is predominant, with cycles of 40 or 50 min achieved in monolayer roller ovens.

Figure 5 depicts the single-firing process [29]. The paste is made primarily of clay, feldspar, sand, carbonates and kaolin. If they come from a natural source, previous mixing is required in most cases to ensure homogeneity. The resultant material from wet milling has a particle size smaller than 200 µm. The suspension obtained is dried by atomisation (spray drying of the ceramic mixture), removing part of the water until optimum humidity (5.5–7%) is reached. The main advantage of this method is the production of spherical, hollow and regular granules, which confer high fluidity to the atomised powders and facilitate mould filling operations and the pressing of large pieces. Green pieces are shaped by mechanical compression of the wet ceramic paste in a mould. Hydraulic presses and pressures of approximately 40 MPa are used. The aim of the drying stage is to decrease humidity to sufficiently low enough levels (0.2–0.5%) to allow the proper execution of the glazing and firing steps.

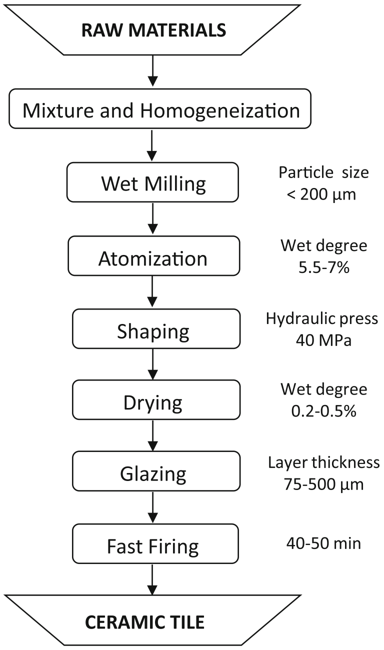

Fig. 5 Manufacturing process diagram of glazed tiles according to a single-firing process

Glazing consists of the application of one or more layers of glaze with a total thickness between 75 and 500 µm, covering the surface of the ceramic tile. This treatment is performed to confer to the fired product a series of technical and aesthetical properties, such as being watertight, cleanable, glossy, coloured, textured and chemically and mechanically resistant.

Like ceramic pastes, glazes are composed of inorganic raw materials. Silica is the main component (i.e. the glass former), although others elements act as fluxes (e.g. alkali, alkaline-earth, boron or zinc), opacifiers (e.g. zirconium or titanium) or dyes (e.g. iron, chromium, cobalt or manganese) are also present. The raw materials commonly employed for glazing (*frits*) are glassy and insoluble in water, prepared from the same crystalline materials, but previously melted around 1500 °C, and then suddenly cooled in water or air. In water-cooling, the melted material is poured directly into water, and due to the thermal shock, glass rupture occurs in small fragments of irregular shapes. In contrast, in air-cooling, the melted mass is passed through two cylinders (cooled inside by air), and a thin, solid and fragile glassy layer that is easily broken into small flakes is obtained. Most of the glazes used in the industrial manufacturing of pavement and covering tiles have a fritted portion of their composition. They may utilise a single frit or a mixture of several.

Finally, the green piece undergoes a specific thermal cycle depending on the type of material desired (i.e. stoneware or porcelain stoneware).

Glass–ceramic glazes

In recent years, pavement and covering ceramic tiles have undergone significant changes. In the 1990s, there was a large increase in demand for tiles with improved and advanced properties, such as high resistance to abrasion, higher hardness, lower closed porosity and improved chemical resistance [25]. For this reason, the possibility of using glass–ceramic glazes was investigated. Until then, only opaque glass–ceramic glazes with zircon or TiO_2 had been developed.

The design of a glass–ceramic glaze must ensure that the precursor frit is technically and commercially compatible with the fabrication conditions normally used in industrial production, where glazes should consolidate in a single heat treatment (fast firing). Densification is achieved by sintering in the presence of a viscous flow at temperatures slightly higher than the glass transition temperature (T_g), resulting in a compact layer nearly free of porosity. Above the T_g, viscosity tends to decrease, and every glassy particle becomes spherical. A liquid phase is formed between particles and, if the temperature is high enough to maintain some degree of viscosity, they start to develop a structural connection by the formation of necks. Nevertheless, it is also fundamental that during this fast-firing cycle, sufficient crystallisation occurs to achieve a glaze with an elevated percentage of the crystalline phase [30]. Rasteiro et al. [25] studied the relationship between the devitrification and sintering processes, determining that the latter always occurs at temperatures higher than T_g, and, when crystallisation begins, sintering stops. Moreover, they state that the softening temperature is always reached after crystallisation begins. The main conclusion drawn is that crystal formation interferes with the frit sintering process in the manufacture of glass–ceramic glazes. Therefore, it is desirable that the densification of the glazed layer be finished by the onset of crystallisation. Thus, dense materials with low porosity and high crystallinity are achieved. However, these processes are not always observed in the ideal sequence because crystallisation can occur before or during sintering.

The characteristics of the glaze surface depend not only on the glaze itself, but also on the nature of the support and their interaction during firing. There are strict requirements in the linear expansion coefficient of the glaze. A consistent seal between the ceramic base and glaze coating must be formed, so it should be very similar to the linear expansion coefficient of the biscuit. The phase composition and structure developed in the heating treatments are important as well. If the linear expansion coefficient of the glaze were smaller than that of the support, it would shrink to a lesser extent, generating compressive forces in the cover and traction forces in the support. If, however, it is greater than that of the support, the opposite effect will occur: the glaze would shrink more than the support during cooling, so the traction and compressive strengths would be reversed. In both cases, the result is similar: thin cracks appear in the surface, resulting in a glaze crazing. In any case, the greater the difference in the thermal expansion of the ceramic support and the glaze, the faster defects will appear. If the forces do not overcome the resistance of the glaze, defects will not appear, but could become visible if the ceramic tile undergoes additional forces. At any rate, a slightly lower expansion coefficient for the glaze is preferred over a higher one. A glassy layer under compressive stress makes the tile more resistant to mechanical strain [31].

The tendency to crystallise and crystallisation rate depend on, among other factors, the chemical composition of the frit. The more similar is the composition of the glass to a silicate-like mineral, which can only be obtained in crystalline form, the faster the crystalline phase will form. For this reason, the most common crystalline phases in glass–ceramic glazes are zircon ($ZrSiO_4$), anorthite ($CaAl_2Si_2O_8$), wollastonite ($CaSiO_3$), celsian ($BaAl_2Si_2O_8$), leucite ($KAlSi_2O_6$), cordierite ($Mg_2Al_4Si_5O_{18}$) and mullite ($Al_6Si_2O_{13}$). Moreover, high concentrations of some oxides, dissolved at high temperatures in the melted glass, can precipitate during cooling in the matrix of this glass, such as TiO_2 in form of rutile crystals or Fe_2O_3 in the form of hematite.

However, the tendency to crystallise during cooling is also determined by the presence or formation of nuclei of crystallisation, which induce great ordering in the glassy structure. These nuclei can be incompletely dissolved particles of the raw materials. Nucleus formation and crystal growth can easily start at phase boundary surfaces (e.g. on the surface of the bubbles or immiscible droplets of a liquid phase), as well as at the surface of the glaze layer.

The simpler the glaze composition, the easier will be its devitrification. The segregation of a crystalline phase may become opaque or cloudy after a transparent initial glass without a great decrease of surface gloss, but it can make the surface matte, irregular and rough [32].

Glaze classification

The classification of glazes presents significant difficulties because it is not easy to ascertain technically rigorous and operational classification criteria. Each criterion used defines a different type of classification, which may or may not be useful, depending on the needs of the interested party. One may select certain aspects of their behaviour in the production process (e.g. fusibility or refractoriness) or of their composition (e.g. the presence of a particular component or systematic classification according to composition). Possible classifications of ceramic glazes (Table 1) are:

- *According to the fusibility*: This is a widely used criterion, but it is insufficient to establish a rigorous glaze classification because the only information included is the melting temperature. Following this criterion, glazes differing widely in appearance and properties would be classified in the same group.
- *According to the presence of some important component*: This classification is restricted to a single component of the glaze, and in some cases is useful, but in other cases is insufficient because it does not provide any type of further information.

Table 1 Glaze classification according different criteria

Criterion	Classification
Fusibility	Fusible
	Hard or less fusible
Presence of an important component	Lead-containing
	Non lead-containing
Further application and firing process	Single-firing covering
	Single-firing pavement
	Double conventional-firing covering
	Double fast-firing covering
Production application	Bases
	Airbrushing (pulverised)
	Pips
	Serigraphy
Effect on the finished product	Shining
	Matte
	Semi-matte
	Satin
	Transparent
	Opaque
	Coloured

- *According to further application*: In the concrete case of industrial fabrication of pavement and covering ceramic tiles, this classification is based on the firing process.
- *According to production application*: This classification is based on the type of application technique using during glazing.
- *According to the effect on the finished glaze*: In this case, a classification may be established based on optical criteria, such as gloss, colour or opacity.

It is evident that one glaze may be classified as belonging to several different groups at the same time. This type of classification, used quite often, can lead to confusion because two same-type glazes can be extraordinarily different in both composition and properties despite being classified in the same group. Another glaze classification scheme was proposed by Parmelee [31], according to the chemical composition of the glaze (Table 2). Although this is not a good scheme from either theoretical or practical points of view, it can be quite useful in understanding glaze composition.

As mentioned in the "Introduction" section, the technological properties and superficial appearance of glass–ceramic glazes are related to the main crystalline phase developed. For this reason, the arrangement of glazes in this review paper is based on the nature of the devitrified crystalline phase. As silicates are the most frequent crystalline phases in glass–ceramic glazes, they have been classified in silicate- and oxide-based glazes. In addition, a section focused on glazes with specific functionalities is also included. Tables 3 and 4 present a summary of mineralogical data and physical features of the most common crystalline phases in glass–ceramic glazes.

Table 2 Ceramic glaze classification according to chemical composition, proposed by Parmelee [31]

	Criterion	Classification
Raw glazes	Lead-containing	With alumina
		Without alumina
	Non lead-containing (with alumina)	With alkaline-earth
		With alkaline and alkaline-earth
		With alkaline, alkaline-earth and ZnO
		With boron
		Salt glazes
Fritted glazes	Lead-containing	With alumina
		Without alumina and boron
	Non lead-containing	With boron
		Without boron
		With high BaO content

Silicate-based glass–ceramic glazes

Silicates are classified in six different categories based on the structure of their silicate group, namely, nesosilicates (isolated (insular) $(SiO_4)^{4-}$ tetrahedra connected only by interstitial cations); sorosilicates (isolated $(Si_2O_7)^{6-}$ double tetrahedra groups); cyclosilicates (linked tetrahedra with $(Si_xO_{3x})^{2x-}$ rings, which exist as 3-member $(Si_3O_9)^{6-}$, 4-member $(Si_4O_{12})^{8-}$ and 6-member $(Si_6O_{18})^{12-}$ rings); inosilicates (interlocked silicate tetrahedra leading to either SiO_3^{2-} single chains or $(Si_4O_{11})^{6-}$ double chains); phylosilicates (parallel sheets of silica and alumina tetrahedral $(Si_2O_5)^{2-}$, $(AlSi_3O_{10})^{5-}$ or $(Al_2Si_2O_{10})^{6-}$) and tectosilicates (three-dimensional frameworks of silicate tetrahedra with formulas of SiO_2, $(AlSi_3O_8)^{1-}$ or $(Al_2Si_2O_8)^{2-}$).

Nesosilicates ($(SiO_4)^{4-}$ tetrahedra)

Zircon ($ZrSiO_4$)–zirconia (ZrO_2) glazes

Zircon and zirconia have long been employed to generate white opaque glaze coatings, which are used in the ceramic tile industry to form a base on which layers of serigraphy can be applied. Opaque glazes have a considerable amount of finely dispersed opacifying crystalline phase exhibiting a noticeable difference in refractive index relative to the glassy matrix. Zircon ($ZrSiO_4$), ZrO_2, ZnO, TiO_2 and SnO_2

Table 3 Summary of mineralogical data of the most common crystalline phases in glass–ceramic glazes (The data shown are collected from Mineralogy Database (http://www.webmineral.com/). Otherwise, the references is indicated)

Classification	Phase	Empirical formula	Crystal system	Space group	Axial ratios	Angles	DRX main peaks (d spacing (Å) (I/I_0))
Nesosilicate	Zircon	$ZrSiO_4$	Tetragonal–ditetragonal dipyramidal	$I\,4_1/amd$	$a{:}c = 1{:}0.91$		3.30 (1), 2.52 (0.45), 4.43 (0.45)
	Willemite	2ZnO·SiO2	Trigonal–rhombohedral	$R\,\bar{3}$	$a{:}c = 1{:}0.67$		2.63 (1), 2.83 (0.95), 3.49 (0.8)
	Mullite	$3Al_2O_3{\cdot}2SiO_2$	Orthorhombic–dipyramidal	Pbam	$a{:}b{:}c = 0.99{:}1{:}0.38$		3.39 (1), 3.43 (0.95), 2.21 (0.6)
Sorosilicate	Akermanite	$2CaO{\cdot}MgO{\cdot}2SiO_2$	Tetragonal–scalenohedron	$P\,\bar{4}\,2_1m$	$a{:}c = 1{:}0.64$		2.87 (1), 1.76 (0.3), 3.09 (0.3)
Cyclosilicate	Cordierite	$2MgO{\cdot}2Al_2O_3{\cdot}5SiO_2$	Orthorhombic–dipyramidal	C ccm	$a{:}b{:}c = 1.74{:}1{:}0.95$		3.13 (1), 8.45 (0.8), 8.54 (0.8)
Inosilicate	Wollastonite	$CaO{\cdot}SiO_2$	Triclinic–Pinacoidal	$P\,\bar{1}$	$a{:}b{:}c = 1.08{:}1{:}0.97$	$\alpha = 90.03°$ $\beta = 95.37°$ $\gamma = 103.43°$	3.31 (1), 3.83 (0.85), 3.52 (0.8)
	Spodumene	$Li_2O{\cdot}Al_2O_3{\cdot}4SiO_2$	Monoclinic	C2/c [33]	$a{:}b{:}c = 1.13{:}1{:}0.62$	$\beta = 110.17°$	2.92 (1), 2.79 (0.9), 4.21 (0.75)
	Diopside	$CaO{\cdot}MgO{\cdot}SiO_2$	Monoclinic–prismatic	C 2/c	$a{:}b{:}c = 1.09{:}1{:}0.59$	$\beta = 105.80°$	2.99 (1), 2.53 (0.4), 2.89 (0.3)
Phyllosilicate	Biotite	$K(Mg,Fe)_3(AlSi_3O_{10})(F,OH)_2$	Monoclinic–prismatic	C 2/m	$a{:}b{:}c = 0.58{:}1{:}1.10$	$\beta = 100.26°$	3.37 (1), 10.10 (1), 2.66 (0.8)
Tectosilicate	Cristobalite	SiO_2	Tetragonal–trapezohedral	$P\,4_12_12$	$a{:}c = 1{:}1.39$		4.05 (1), 2.49 (0.2), 2.84 (0.13)
	Anorthite	$CaO{\cdot}Al_2O_3{\cdot}2SiO_2$	Triclinic–pinacoidal	$P\,\bar{1}/I\,\bar{1}$	$a{:}b{:}c = 0.64{:}1{:}1.10$	$\alpha = 93.17°$ $\beta = 115.85°$ $\gamma = 91.22°$	3.20 (1), 3.18 (0.75), 4.04 (0.6)
	Leucite	$KAl(Si_2O_6)$	Tetragonal–dipyramidal	$I\,4_1/a$	$a{:}c = 1{:}1.05$		3.27 (1), 3.44 (0.85), 5.39 (0.8)
Simple Oxides	Zirconia	ZrO_2	Monoclinic [34]	$P\,2_1/c$ [35]	$a{:}b{:}c = 0.99{:}1{:}1.02$ [35]	$\beta = 99.23$ [35]	3.16 (1), 2.83 (0.8), 2.61 (0.6)
			Tetragonal [34]	$P\,4_2/nmc$ [35]	$a{:}c = 1{:}1.44$ [35]		2.95 (1), 1.81 (0.32), 1.53 (0.2)
			Cubic [34]	$Fm\,\bar{3}m$ [35]	$a = 5.09$ [35]		2.96 (1), 1.81 (0.32), 2.56 (0.17)
	Anatase	TiO_2	Tetragonal–ditetragonal Dipyramidal	$I\,4_1/amd$	$a{:}c = 1{:}2.51$		3.51 (1), 1.89 (0.33), 2.38(0.22)
	Rutile	TiO_2	Tetragonal–ditetragonal Dipyramidal	$P\,4_2/mnm$	$a{:}c = 1{:}0.64$		3.25 (1), 1.69 (0.5), 2.49(0.41)
	Hematite	Fe_2O_3	Trigonal–hexagonal Scalenohedral	R 3c	$a{:}c = 1{:}2.73$		2.69 (1), 1.69 (0.6), 2.51(0.5)
Multiple Oxides	Spinel	$MgO{\cdot}Al_2O_3$	Isometric–hexoctahedral	F d3m	$a = 8.08$		2.44 (1), 2.02 (0.7), 1.43 (0.6)
	Gahnite	$ZnO{\cdot}Al_2O_3$	Isometric–hexoctahedral	F d3m	$a = 8.06$		2.44 (1), 2.86 (0.84), 1.43(0.43)
	Franklinite	$ZnO{\cdot}Fe_2O_3$	Isometric–hexoctahedral	F d3m	$a = 8.42$		2.55 (1), 1.50 (0.8), 2.99 (0.7)

Monoclinic Low-temperature phase, *Tetragonal* Between 1440–2640 K, *Cubic* High-temperature phase

Table 4 Summary of physical features of the most common crystalline phases in glass–ceramic glazes (The data shown are collected from Mineralogy Database (http://www.webmineral.com/). Otherwise, the references is indicated)

Classification	Phase	Empirical formula	Hardness (Mohs)	Density (g/cm^3)	Habit/crystal shape	Refraction index (n)	Expansion coefficient ($\times 10^{-7}$) (°C^{-1})	Luminescence
Nesosilicate	Zircon	$ZrSiO_4$	7.5	4.65	Slender prisms-tabular	1.92–1.97	46 (up to the change) [36]	Fluorescent
	Willemite	$2ZnO{\cdot}SiO_2$	5.5	4.05	Prismatic-Slender prisms	1.67–1.73	32 (20–1000 °C) [15]	Fluorescent and phosphorescent
	Mullite	$3Al_2O_3.2SiO_2$	6–7	3.05	Slender prisms	1.62–1.66	53 (20–1000 °C) [15]	–
Sorosilicate	Akermanite	$2CaO{\cdot}MgO{\cdot}2SiO_2$	5–6	2.94	Short prismatic to thin tabular; commonly massive granular [37]	1.61	45 (25–1300 °C) [38]	Fluorescent [47, 48]
Cyclosilicate	Cordierite	$2MgO{\cdot}2Al_2O_3{\cdot}5SiO_2$	7	2.65	Slender prisms	1.51–1.57	6 (100–200 °C) [15]	–
Inosilicate	Wollastonite	$CaO{\cdot}SiO_2$	5	2.84	Fibrous-radial habit	1.59–1.61	94 (100–200 °C) [15]	–
	Spodumene	$Li_2O{\cdot}Al_2O_3{\cdot}4SiO_2$	6.5–7	3.15	Prismatic [37]	1.67–1.69	9 (20–1000 °C) [15]	–
	Diopside	$CaO{\cdot}MgO{\cdot}SiO_2$	6	3.40	Slender prisms	1.67–1.73	$\alpha1 = 77$ $\alpha2 = 173$ $\alpha3 = 70$ [39]	–
Phyllosilicate	Biotite	$K(Mg,Fe)_3(AlSi_3O_{10})(F,OH)_2$	2.5–3	3.09	Lamellar–micaceous	1.58–1.70	173 parallel to c-axis, 96.5 perpendicular to c-axis [40]	–
Tectosilicate	Cristobalite	SiO_2	6.5	2.27	Spherical, rounded aggregates	1.47–1.48	500 (20–300 °C) [15]	Fluorescent
	Anorthite	$CaO{\cdot}Al_2O_3{\cdot}2SiO_2$	6	2.73	Euhedral crystals–striated	1.57	45 (100–200 °C) [15]	–
	Leucite	$KAl(Si_2O_6)$	6	2.47	Euhedral pseudocubic crystals	1.50–1.51	200 (20–600 °C) [41]	–
Simple Oxides	Zirconia	ZrO_2 Monoclinic	6.5	5.75	Tabular	2.16–2.27	n/r	–
		Tetragonal	6.5	6.13 [42]	n/r	n/r	n/r	Fluorescent [49, 50]
		Cubic	8	6.16 [42]	Dipyramidal prismatic [43]	2.18 [43]	n/r	Fluorescent
	Anatase	TiO_2	5.5–6	3.89	Pyramidal-tabular	2.52–2.53	272 (20–1000 °C) [44]	–
	Rutile	TiO_2	6–6.5	4.25	Acicular-slender prisms	2.67	291 (20–1000 °C) [44]	–
	Hematite	Fe_2O_3	6.5	5.30	Tabular	2.66-2.67	80 (250 °C) [45] 110 (450 °C) [45]	–
Multiple Oxides	Spinel	$MgO{\cdot}Al_2O_3$	8	3.64	Euhedral crystals	1.73–1.76	76 [46]	Sometimes fluorescent
	Gahnite	$ZnO{\cdot}Al_2O_3$	8	4.30	Euhedral crystals-striated	1.74–1.86	72 (20–1300 °C) [15]	–
	Franklinite	$ZnO{\cdot}Fe_2O_3$	5.5–6	5.14	Euhedral–large masses crystals	2.35–2.40	n/r	–

n/r not reported

are well known opacifying agents used to produce opaque glazes.

Opacifiers provide opacity to the glaze by scattering and reflecting the light that is incident on the coating. The factors that control the opacity in glazes include the difference in refractive index between the glass and opacifier, the number, size, shape and distribution of the opacifier particles, the incident light wavelength and the glaze thickness. Because finer materials contain significantly more particles for a given unit weight, finer opacifier grades produce high opacity glasses [51]. The maximum light scattering and whiteness with zircon occur with a particle size range of 0.60–0.75 μm and a mass fraction of 0.16 [52, 53].

There are two general methods of dispersing particles in glazes. The first is mechanical dispersion by wet grinding of the whole glaze composition containing the fine powder opacifier. In this case, the crystalline phase must be stable enough to be protected from glass attack at high temperatures. The second method is dissolution and controlled precipitation inside the glassy phase [54], to promote the nucleation and growth of nanosized crystallites.

Amongst commercial frits, those containing zircon and zirconia are of great interest because of the effect that phase transformations of ZrO_2 can produce in glazes. $ZrSiO_4$ gives rise to opaque frits, which are commonly designated as ‘white of zirconium’. These frits, which are glossy, opaque, viscous and with low fusibility, are composed of 50–60 SiO_2, 8–14 ZrO_2 (wt%), fluxing elements such as Na_2O, K_2O, PbO and B_2O_3 (20–25%) as major components and stabilising elements such as ZnO, Al_2O_3, CaO, BaO and MgO as minor components (7–9% maximum) [55].

Regardless of the type of zirconium-bearing opacifier used, $ZrSiO_4$ is the main crystalline phase promoting opacity and whiteness in zirconium glazes [56]. However, it has been established that (i) a threshold amount of zircon is required before opacity is observed and (ii) large amounts of zircon are required to achieve adequate opacity. More than three times the amount of zircon is needed to obtain adequate opacity, compared with traditional opacifiers such as titania and tin oxide [57]. In zircon glazes, opacity occurs through the partial solubility of zirconium-bearing components in the silicate melt and crystallisation of zircon in cooling from ZrO_2 and SiO_2. The resulting zircon crystals have a significantly higher index of refraction (2.05–2.40) than the glassy matrix (1.50–1.70) and thus effectively scatter light [32]. Therefore, the boundaries between translucent and opaque glazes are isotherms of ZrO_2 solubility in the melt [58].

In general, there are two ways to introduce $ZrSiO_4$ into a glaze. The first is to formulate the composition of the glaze from frits containing ZrO_2. The second is to use $ZrSiO_4$ as an additive in the glaze composition. In this case, it may be formulated from either a ZrO_2-containing or a ZrO_2-free frit.

The use of $ZrSiO_4$ as glaze opacifier has become conventional in the ceramic glaze industry and several research have reported the influence of frit composition on the solubility of zirconium compounds. In zirconia-bearing frits, the amount of zircon or zirconium oxide that initially forms is dependent on the SiO_2:ZrO_2 ratio in the frit [59]. Frits with lower silica contents initially produce zirconium oxide phases, whereas higher silica glazes initially produce zircon crystals during heating. In both cases, however, zircon is the major opacifying phase in the final glaze [56, 59].

Zirconium dissolution in the melt is also dependent on the viscosity of the silicate melt. El-Defrawi et al. [60] reported on the microchemistry and microstructure of semi-industrially prepared double- (DF) and once-fired (OF) glazed tiles with ZrO_2 contents in the ranges of 6.97–7.70 wt% in DF glazes and 8.51–13.22 wt% in OF glazes, whereas ZnO was 1.90–9.97 and 7.46-13.10 wt% in DF and OF glazes, respectively. The acid/base ratio SiO_2/(R_2O + RO) for all samples ranges was between 1.93 and 4.18. The presence of very high B_2O_3 content (13.30 wt%) minimises the size of zircon grains by their dissolution in a B_2O_3-rich glassy phase. Higher CaO (7–11 wt%), ZnO (9–13 wt%) and Na_2O content (6–8.6 wt%) lead to a decrease in the acid/base ratio to 2, which in turn enhances fluidity (lower viscosity values) during melting. Hence, ionic diffusion accelerates in the glaze melt and such silicates phases as anorthitic plagioclase s.s. ((Na, Ca)$AlSi_3O_8$) and (Na_2O, Zn)-zirconium alumino silicate s.s. recrystallise during cooling at the expense of $ZrSiO_4$. On the other hand, low B_2O_3 content leads to the segregation of a zircon-rich layer at the glaze surface, which decreases the gloss of the glaze.

The study of $ZrSiO_4$ crystallisation in glazes from ZrO_2-containing frits has been of great interest, as the whiteness index of the glaze is related to both the number and size of zircon crystals. Aparici et al. [61] analysed the effect of the firing cycle on the whiteness of a glaze from a frit with 11.5 ZrO_2 and 57.9 SiO_2 (wt%). The only crystalline phase present in this glaze was $ZrSiO_4$, with the formation occurring during heating. The crystallised volume fraction of zircon (x_c) increased with temperature, reaching a maximum at 1000 °C. At higher temperatures, x_c decreased slightly, indicating partial dissolution of $ZrSiO_4$ in the glassy phase. In the best case, the zircon crystallised during firing reached 95% of the amount that could be formed if all the ZrO_2 included in the frit composition crystallised as $ZrSiO_4$. The authors pointed out a direct proportionality between the volume fraction of crystals and the whiteness index of the glaze.

Castilone et al. [62] examined the crystallisation of zircon as a function of both the amount of zircon added to the glaze and temperature in glazes containing both zircon and zirconia additions. In glazes with zircon additions, the quantity of zircon that crystallised is a function of the amount of zircon added to the glaze. At zircon additions lower than 3 wt%, most of the $ZrSiO_4$ is dissolved into the melt and is not subsequently recrystallised in the glaze. Between 3 and $\sim$13 wt% added $ZrSiO_4$, more zircon is crystallised in proportion to the amount added. At zircon addition levels >13 wt%, all the $ZrSiO_4$ is crystallised (Fig. 6). The authors pointed out that through heating, a portion of the zircon dissolves and recrystallises afterwards. The dissolved ZrO_2 combines with SiO_2 to recrystallise as zircon in the glaze, using undissolved zircon crystals as seeds. This recrystallisation does not occur in glazes with low concentrations of added zircon, due to the complete dissolution of $ZrSiO_4$, which eliminates the zircon seeds. Thus, the tendency for recrystallisation of zircon from the melt is eliminated. The complete zircon crystallisation may also be attributed to a problem of diffusion distances and the homogeneity of the zirconium-ion distribution throughout the glaze, as suggested by Amorós et al. [63].

When zircon in the glaze results from zirconia additions to the batch, much of the zirconia appears to remain dissolved in the glassy phase and the crystalline zircon formed in the final glaze is lower than expected, even at high zirconia contents. For example, only 9% of crystalline zircon was formed in the final glaze when zirconia and silica were added to the batch to yield 13% zircon. Castilone et al. [62] also acknowledged the strong influence of the type of zirconium-bearing opacifier used on the morphology of zircon crystals formed; thus, low aspect ratio crystals are observed from zircon additions, whereas elongated zircon crystals form from zirconia additions. The increased length of these crystals—close to 10 μm—can lead to a decrease in opacity. The evolution of the number and size of zircon crystals with temperature has also been studied by Ssifaoui et al. [64] in glazes resulting from additions of zircon powder (average size of 2.3 μm) to a frit without ZrO_2. As temperature increases, a considerable amount of zircon is gradually dissolved in the glaze and as a result of firing temperature and time, a large growth of zircon crystallites is observed. This gives rise to a decrease in the number of crystals. The average crystal size increased significantly with increasing time and firing temperature. The authors proposed that zircon crystallised by means of a mechanism of zircon transport between grains through the melt. The proposed mechanism involves several successive stages, namely grain dissolution in the liquid phase, material transport by diffusion through the melt and recrystallisation at the grain surface, which favours the growth of larger grains by an Ostwald ripening mechanism.

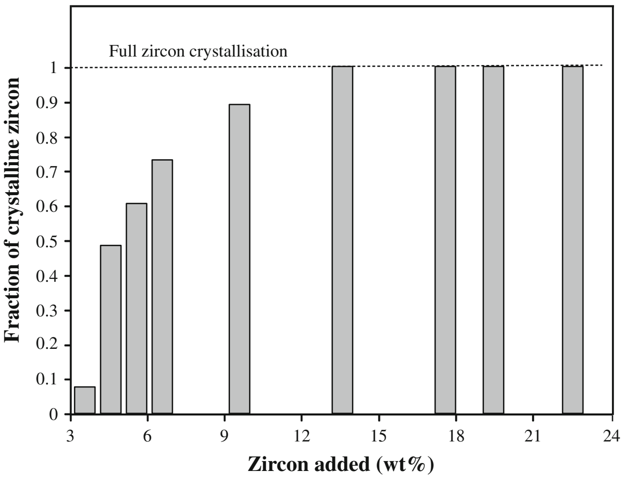

Fig. 6 Amount of crystalline zircon (measured via powder XRD of (312) zircon peak) in the glaze versus the amount of zircon added. Zircon is dissolved at low zircon additions but is fully crystallized at higher zircon contents (Figure drawn from the data shown in [62])

A significant goal in zircon glaze research has been the development of glaze compositions with decreased boron anhydride content, due to the high cost of boron-containing materials. However, boron anhydride is a necessary component of glaze glasses because it is an exceptional flux that ensures a low melting point along with a significant decrease in the thermal expansion coefficient. Bobkova et al. [65] studied the synthesis of opacified zirconium-containing glazes from frits with 4 mol% ZrO_2 and a B_2O_3 content in the range of 7.5–15.0 mol%. Low B_2O_3 content (7.5 mol%) leads to glasses with liquid phase separation, which has been studied by IR spectroscopy. The main absorption corresponding to $[SiO_4]$ groups splits into two bands, corresponding to high-silica ($1080\ cm^{-1}$) and low-silica ($1020\ cm^{-1}$) liquid phases. Phase separation is increased in the range 700–750 °C by the formation of low-silica calcium borate drops in an aluminosilicate matrix, which also include sodium cations. In these glazes, anorthite ($CaAl_2Si_2O_8$) is the first phase that crystallises at 750 °C. Ruffite (tetragonal ZrO_2), the first zirconium-containing phase, is formed at 800 °C but rapidly increases from 800 to 900–950 °C. When zircon crystallises out in the glaze, the content of ruffite is suddenly reduced because $ZrSiO_4$ is formed as result of the reaction between the ZrO_2 and SiO_2 from the residual glassy phase. The authors indicated that the formation of zircon in low-boron glazes consisted of three stages: phase separation of glass, formation of tetragonal ZrO_2 and crystallisation of zircon.

Another important aim in zircon glaze research has been to formulate glaze compositions with reduced zircon content. There is no doubt that zircon is the main opacifier agent used in the ceramic tile industry. ZrO_2-containing glazes are used on floor and wall tiles not only because of their high whiteness and opacity, but also because of the good mechanical and chemical properties imparted to the glazes, which also are well suited to industrial firing cycles. However, the high cost of zircon limits its wide use in relevant glaze compositions. Karasu et al. [66] reported a study aiming to increase the opacity of opaque glaze by reducing the silica/alumina content and replacing sodium feldspar with potassium feldspar in a frit composition with 10 wt% ZrO_2 and 3 wt% ZnO. This change in the glaze composition results in the precipitation of zircon together with larger amounts of other crystalline phases such as anorthite ($CaO\cdot Al_2O_3\cdot 2SiO_2$) and gahnite ($ZnO\cdot Al_2O_3$), which contribute to opacity. The authors concluded that zircon additions to the glaze are not necessary and also that each glaze has a saturation point for zircon content beyond which zircon addition is not effective in the further development of opacity. For optimum opacity, an alumina/silica ratio of 0.26 was identified, whereas the replacement of sodium feldspar by potassium feldspar increased the glossiness of the glaze surface.

The use of nucleating agents to promote $ZrSiO_4$ crystallisation in zirconium glazes has also been taken in consideration. Romero et al. [54] investigated the effects of iron oxide on crystallisation behaviour of a frit with a ZrO_2 content in the range of 6.47–12.93 wt% and Fe_2O_3 in the range of 0.00–8.89 wt%. They reported that the inclusion of Fe_2O_3 does not promote zircon crystallisation. On the contrary, it gives rise to the formation of small rounded crystals of an iron-zinc ferrite, which act as nucleating sites for the crystallisation a new phase consisting of feather-like crystals of diopside ($CaO\cdot MgO\cdot 2SiO_2$).

As has seen so far, zircon is the main opacifier used in the production of opaque ceramic glazes. However, sometimes the presence of zircon is required to maintain the high chemical resistance of the glaze, but a high degree of opacification is not desirable. Vicent et al. [67] addressed the possibility of modifying the opacity in zircon glazes by small additions of opacification inhibiting agents, such as volatile fluorides (NaF, LiF), non-volatile fluorides (Na_3AlF_6, Ba_2F) and thermally stable carbonates (Li_2CO_3, $SrCO_3$). Volatile fluorides lowered the glass transition temperature and induced the crystallisation of small crystals (smaller than 500 nm) that did not increase opacification. The gases released gave rise to pinholing and reduced hardness. The addition of non-volatile fluorides inhibited opacification by producing microcrystal groupings in larger sized clusters. The resulting materials exhibited higher scratch hardness, as well as elevated gloss and transparency. Li_2CO_3 was found to be a potent devitrification inhibitor, decreasing zircon crystallisation as added Li_2CO_3 increased. However, gloss, transparency and glaze hardness were maintained or enhanced with carbonate additions. The joint addition of devitrifying agents (WO_3, Al_2O_3 and MgO) and nucleants by immiscibility (ZrO_2) inhibited opacification without interfering with the devitrification processes.

As frits have evolved to provide better-performing ceramic glazes in both technical and aesthetic characteristics, the number and variety of instrumental techniques used for the study and characterisation of glazes has also increased. Ruiz et al. [68] performed a structural study of glazes from frits containing up to 15 wt% zirconia by FT-Raman spectroscopy. The study of the Q^n group, where n ($n = 0$–4) indicates the number of bridge oxygens in the SiO_4 tetrahedron Q, showed that the glassy network breaks down with an increasing percentage of ZrO_2. This causes an increase in non-bridging oxygen bridge revealed by the increase in Q^0 and Q^1 structural groups and a decrease in Q^2, Q^3 and Q^4 groups. This variation is very significant for ZrO_2 content up to 5%, above which the variations in Q^n units are smaller. The characteristic bands of zircon increase linearly with increasing amounts of crystallised $ZrSiO_4$ in the glaze, indicating the general potential for using FT-Raman spectroscopy to quantify the amount of crystalline phase in ceramic glazes.

When zirconia is added to the batch composition, monoclinic zirconia (m-ZrO_2, or baddeleyite) is commonly employed. Concerning the use of stabilised tetragonal zirconia (t-ZrO_2), instead of monoclinic zirconia, several investigations have been carried out with the aim of enhancing the hardness and/or strength of ceramic glazes. Monrós et al. [69] introduced Ca-partially stabilised zirconia (Ca-PSZ) obtained by sol–gel procedures in the formulation of conventional ceramic glazes and Generali et al. [70] reported the use of t-ZrO_2 in glazes from the M_2O–CaO–ZrO_2–SiO_2 glass–ceramic system (with M = Li, Na and K). These investigations pointed out the low stability of tetragonal zirconia, which promptly reacted with the molten glaze during firing, being dissolved and incorporated into the glassy phase. Direct addition of Ca-PSZ only stabilised cubic zirconia in large additions (15 wt%) and in low volume fractions. Llusar et al. [71] explored the use of yttrium-stabilised polycrystalline tetragonal zirconia (3Y–TZP) as a mechanically reinforcing additive for conventional single-firing ceramic glazes. For 3Y–TZP doped coatings, significant zircon crystallisation occurred (Fig. 7) and stable crystals of tetragonal zirconia were only dominant for large additions (30 wt%). The addition of 3Y–TZP or zircon crystals increased all the relevant mechanical parameters (Hv and K_{IC}). Moreover, the achieved reinforcement was considerably higher in samples with 3Y–TZP than in samples with added zircon, and must be attributed to the beneficial effect of the stress-induced transformation-toughening mechanism produced by the stabilised t-ZrO_2.

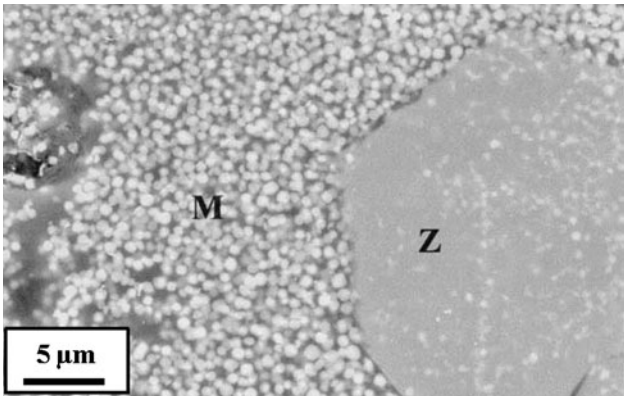

Fig. 7 SEM micrographs of glazes from glossy opaque fired at 1100 °C showing zircon crystallization (Z) and tetragonal zirconia grains (M) [71]

Besides its use as an opacifier in glazes, the ceramic tile industry also employs zircon in pigment formulation. Zircon-doped pigments are the most stable ceramic colourants up to 1200 °C [57, 72]. Zircon's tetragonal structure has the ability to accommodate vanadium, iron and praseodymium, and its high chemical and thermal stability make it ideal for use in ceramic coatings [73]. Zircon pigments are normally added to glaze batches in the range of 0.1–5.0% by weight, and their solubility during firing varies with the frit composition. Earl et al. [74] explored the dissolution and crystallisation of zircon–vanadium (Zr–V) blue pigments in both glossy opaque (with 8 wt% ZrO_2) and transparent (without ZrO_2) glazes. In ZrO_2-containing frits, zircon was the only crystalline phase detected in glazes, where, in addition to zircon pigment, small spherical ($\leq$0.5 mm) zircon crystals and fibrous zircon crystallised during firing. The authors stated that both pigment and zircon needles were aligned with the glaze surface, which indeed was also observed by Concepcion et al. [75] in a study of the interaction of different ZrO_2 particles with glass frits and by Sorlí et al. [76] in glazes of the ZnO_2–CaO–Al_2O_3–SiO_2 system including 5.0 wt% ZrO_2 in the frit composition.

Frits with ZrO_2 provide the best high-temperature stability for both opaque and transparent glazes with zircon pigments by lowering the solubility of zircon and crystallisation above 1000 °C. An increase in the Al_2O_3:alkali ratio in ZrO_2-containing frits leads to higher zircon crystallisation and results in finer spherical zircon precipitates, which improve glaze opacity and whiteness. Glazes from frits without ZrO_2 contained some Zr-V pigment crystals. However, crystallisation of non-zirconium species was prominent and caused significant microstructural instability and loss of colour and gloss. The presence of ZnO in the frit promotes zircon precipitation and results in highly opacified glazes. Substituting SrO for ZnO restrains zircon crystallisation and allows for the formation of stable transparent glazes with high levels of ZrO_2.

Schabbach et al. [72] evaluated the influence of firing temperature on the colour developed by a blue vanadium–zircon pigment in an opaque ceramic glaze with 7.40 wt% ZrO_2. They concluded that changes in the grain size and morphology (aspect ratio) of zircon crystals formed during firing contributed significantly in the scattering of the light and glazes with higher amounts of crystallised zircon phase show a lower reflectance curve due to the greater aspect ratio of the zircon crystals.

Willemite (Zn_2SiO_4)–gahnite ($ZnAl_2O_4$) glazes

ZnO is frequently used in glaze compositions because it decreases the viscosity and surface tension of the glaze melt, which favours the spreading of the melt over the substrate and promotes the formation of a high-quality glaze coating. Moreover, it also has a positive effect on the shine and chemical resistance of the glaze. But in addition to the benefits of ZnO incorporation in the glaze composition, in terms of improving the physical and chemical properties of glazes, ZnO also plays an important role in the development of glass–ceramics glazes. Zinc oxide reacts with SiO_2 or Al_2O_3 in a melt to form fine crystals of gahnite ($ZnO{\cdot}Al_2O_3$) upon cooling, which act as an opacifying agent, and/or large crystals of willemite ($2ZnO{\cdot}SiO_2$), which contribute unique ornamental effect to the glaze. Whereas the size of the gahnite crystals is around 1 µm, the size of willemite crystals reaches 30–80 µm, and in some cases, they can be significantly larger [77].

Zinc-based compositions are widely used for glazing soft porcelain and ornamental ceramics [78, 79], and the kinetics of the processes of seed formation and growth of willemite and gahnite crystals in such materials has been widely reported [80–82]. Willemite crystals exhibit different morphologies, varying with the viscosity of the melt, which is dependent on the glaze composition and crystal growth temperature. Thus, for a specific glaze composition, at high temperatures (1160–1190 °C), willemite grows as isolated acicular crystals, but as the temperature decreases (1100–1160 °C), the viscosity of the melt increases and subsequently, the monocrystals split with formation of two-leaf spherulites. At lower temperatures (980–1100 °C), the greater viscosity of the melt induces monocrystals to split more perfectly, which leads to the formation of rounded spherulites [77].

Takashima [83] studied the behaviour of Cr^{3+} and Fe^{3+} ions in a glaze of composition $0.2(K,Na)_2O$–0.2CaO–0.6ZnO–xAl_2O_3–xCr_2O_3–(or Fe_2O_3)–2.0 SiO_2 with $x =$ 0.01, 0.02, 0.04, 0.08 and 0.16 with gahnite crystallisation. Almost all of the Cr_2O_3 added to the glaze migrated into the gahnite crystals. In the case of Fe_2O_3, the number of

Fe^{3+} ions that migrated to the gahnite phase was lower than that of Cr^{3+} ions in the analogous glaze, and gahnite formation was reduced as the Fe_2O_3 content increased in the glazes. Similarly, Karasu and Turan [84] investigated the effect of different colouring agent additions on crystal development in zinc-containing soft porcelain glazes. The authors pointed out that when CoO and TiO_2 are used as colouring oxides, both willemite and gahnite crystallise simultaneously, whereas MnO_2 inhibited gahnite formation and promoted willemite formation. Others colouring agents, such as CuO, assisted or hindered gahnite crystallisation depending on the crystal growth temperature. Sun et al. [85] studied a willemite ware glaze of composition 28.3 ZnO, 51.2 SiO_2, 4.1 TiO_2, 5.4 Na_2O, 2.5 K_2O, 4.1 CaO, 3.3 FeO and 1.1 Al_2O_3 (mol%) by reflective confocal microscopy in order to achieve a better understanding of the relationship between the microstructure and the aesthetic qualities of these glazes. The study highlighted that crystallisation occurs through a two-stage amorphous phase separation, first spinodal-like decomposition as (Zn, Ti, Ca)-rich and (Si, Al, K, Na)-rich regions, and then nucleation of willemite crystallites and amorphous droplets, respectively, which are responsible for the jade-like lustre exhibited by the glaze.

The investigations of willemite–gahnite glazes described here correspond to glazes over porcelain or traditional ceramic, which are obtained by firing cycles at higher temperatures and longer times than those traditionally used in manufacturing ceramic tile. Despite its aesthetic qualities, few references report the fast firing of willemite–gahnite glazes. Sorlí et al. [76] analysed the mechanical and optical relation between composition, microstructure and properties of a family of glossy white ceramic glazes of the ZnO–CaO–SiO_2 system. Glazes with high proportions of ZnO and Al_2O_3 and the presence of alkaline fluxes enabled devitrification of willemite, anorthite, gahnite or a mixture of the three crystalline phases. Anorthite devitrification was always accompanied by gahnite. In addition, depending on the firing cycle, gahnite could retain residual anorthite crystals. Gahnite exhibited a homogeneous microstructure composed of nanoparticles (400–600 nm). In contrast, anorthite showed clustered crystallisations around glaze particle interfaces. Eftekhari Yekta et al. [86] reported studies of glass–ceramic glazes in the ZnO–Al_2O_3–SiO_2–ZrO_2 system to improve the surface quality and micro-hardness of floor tile glazes by precipitation of hard gahnite and zirconium silicate phases. To this end, calcium and magnesium oxides in a glaze with composition 55.35 SiO_2, 7.32 Al_2O_3, 11.07 CaO, 7.50 MgO, 9.54 ZrO_2, 1.02 Na_2O, 2.62 K_2O and 5.58 B_2O_3 (wt%) were progressively substituted by zinc oxide, while keeping the Al_2O_3/ZnO molar ratio constant. During firing, a fine microstructure composed of cubic gahnite and fibrous zirconium silicate particles immersed in glass matrix developed. However, the addition of a small amount of Li_2O (2.5 wt%) led to precipitation of β-quartz solid solution and willemite, decreasing the amount of gahnite crystallised from the melt. The studied gahnite-based glazes showed higher micro-hardness values than traditional floor tile glazes. More recently, Bou et al. [87] have examined how the specific surface area (SSA) of alumina particles affects the technical and aesthetic properties of a glaze from a mixture composed of 80 wt% of a frit composition in the ZnO–CaO–Al_2O_3–SiO_2 system used in industry to produce transparent and glossy glazes, 7% kaolin and 13% alumina. Alumina particles with low SSA did not dissolve and hardly reacted with the glassy phase. In contrast, high SSA alumina (>7 m^2/g) reacted with the glassy phase to form gahnite by diffusion of the zinc oxide contained in the glassy phase within the alumina particles.

Mullite ($Al_6Si_2O_{13}$) glazes

Mullite-based glass–ceramic materials have attracted much attention in recent years because mullite ($3Al_2O_3\cdot 2SiO_2$) is characterised by excellent mechanical, creep, thermal and chemical properties.

Torres et al. [88] studied the feasibility of developing spinel glass–ceramic glazes in the ZnO–MgO–B_2O_3–Al_2O_3–SiO_2 system. They highlighted that the addition of B_2O_3 as flux favoured the crystallisation of mullite as the main crystalline phase in the glaze. Based on these results, the authors considered the possibility of obtaining mullite-based glass–ceramic glazes by substitution of increasing amounts of Al_2O_3 by B_2O_3 in a parent glass with composition 53 SiO_2, 35 Al_2O_3, 9 MgO and 3 CaO (wt%) located in the mullite primary crystallisation field of the CaO–MgO–Al_2O_3–SiO_2 quaternary system [89, 90]. The results of the investigations showed again that B_2O_3 favoured mullite crystallisation and thus, higher amounts of boron oxide led to increased formation of primary phase mullite. Mullite formation in these glazes occurs through a phase separation process (Fig. 8a) favoured by the limited solubility of B_2O_3 in some aluminosilicate glasses, promoting the development of ordered zones with high alumina content [91]. At the beginning of the crystallisation process, small aggregates of needle-like crystals are formed in the early surface of particles (Fig. 8b). Upon increasing the final temperature, the number of aggregates of mullite crystals increases and an almost continuous distribution of mullite crystal occurred all around the surface of particles (Fig. 8c). The amount of mullite phase developed in the glaze containing 9 wt% B_2O_3 was 19.5 wt% and the final microstructure of the glass–ceramic glaze showed the formation of well-shaped, long acicular mullite crystals dispersed within the residual glassy phase.

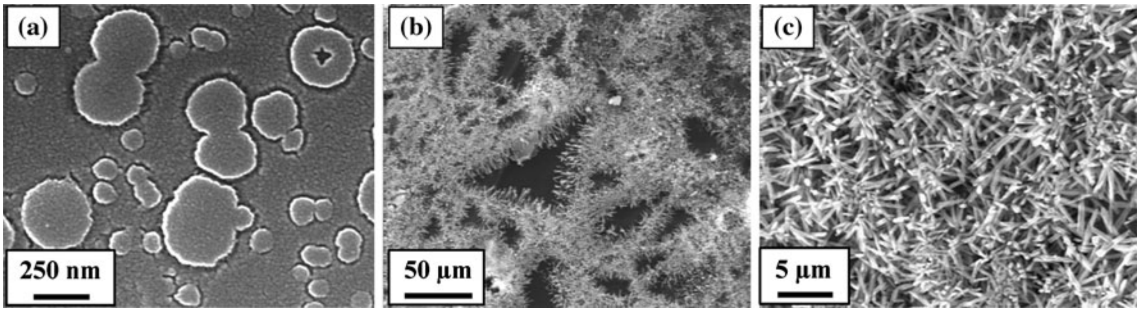

Fig. 8 Crystallization sequence in a glaze of composition 53 SiO_2, 24 Al_2O_3, 9 MgO, 3 CaO and 9 B_2O_3 (wt%) showing **a** phase separation after fast heating at 800 °C for 5 min; **b** aggregates of needle-like mullite crystals growing from the surface to the center of glass particles; and **c** interlocked mullite crystals after fast heating at 1160 °C for 5 min [88, 89]

Sorosilicates ($(Si_2O_7)^{6-}$ dimers)

Akermanite ($Ca_2MgSi_2O_7$) glazes

Akermanite ($2CaO{\cdot}MgO{\cdot}2SiO_2$) is reported by Bou et al. [87] to be found in glazes prepared by adding alumina with a high specific surface area (75 m^2/g) to a frit composed of 58 SiO_2, 3 B_2O_3, 6 Al_2O_3, 12 CaO, 3% MgO, 11 ZnO and 5 K_2O (wt%). Akermanite development is attributed to the reaction between alumina particles and the glassy phase stemming from the frit.

Cyclosilicates ($(Si_xO_{3x})^{2x-}$ rings)

Cordierite ($Mg_2Al_4Si_5O_{18}$) glazes

Glass–ceramics containing cordierite ($2MgO{\cdot}2Al_2O_3{\cdot}5SiO_2$) are known for their special properties such as thermal stability and thermal shock resistance, high mechanical strength and exceptional dielectric properties. Cordierite can crystallise in three different polymorphs: orthorhombic β-cordierite (low temperature), hexagonal α-cordierite (high temperature) and the metastable form μ-cordierite.

Crystallisation in cordierite-based glasses has a tendency to occur mostly by a surface nucleation mechanism [92, 93]. However, nucleating agents play an important role in crystallisation, as depending on the concentration of nucleant in the glass, the crystallisation mechanism changes. Thus, De Vekey and Majumdar [94] found that for glasses in the cordierite primary phase field of the CaO–MgO–Al_2O_3–SiO_2 system, for concentrations of TiO_2 lower than 7 wt%, crystallisation starts from the surface. Once this limit is exceeded, volume or bulk crystallisation becomes the predominant mode.

The MgO:Al_2O_3:SiO_2 ratio in MgO–Al_2O_3–SiO_2 glasses strongly affects the crystallisation of μ- and α-cordierite [95].The formation of μ-cordierite is suppressed, and the crystallisation of the α- form is enhanced in glasses richer in MgO and SiO_2 relative to stoichiometric cordierite. Moreover, studies on the effect of oxide additions on the crystallisation behaviour of $2MgO{\cdot}2Al_2O_3{\cdot}5SiO_2$ glasses suggest that B_2O_3 and/or TiO_2 additions prevent the formation of μ-cordierite [96].

Glass crystallisation in the MgO–Al_2O_3–SiO_2 system is an extremely complex process because of the high number of phases, many of which are metastable, that can crystallise from such a glass. The chemical and mechanical properties of the crystals and residual glassy phases in this system, along with the low cost of raw materials, make this an attractive system for the glazing of tiles. Moreover, commonly used nucleating oxides such as TiO_2, and ZrO_2, when added to this system, allow the control of the glass/crystal ratio and the crystallite size and shape [97].

Ferrari et al. [98] first reported on the possibility of using cordierite glass–ceramics as tile glazes. They selected several glass compositions able to crystallise cordierite ($2MgO{\cdot}2Al_2O_3{\cdot}5SiO_2$) as the major crystalline phase after a controlled devitrification process and studied their ability to be used as tile glaze components, based on industrial borosilicate frits. TiO_2 (8–9%) and CaO (5%) were added to some compositions as nucleating agents. Nucleating agents led to reduced T_g values, which also decreased when the ratio $SiO_2/(Al_2O_3 + MgO)$ in frit compositions was diminished. However, nucleating agents considerably affected both the crystallisation mechanism and the crystalline phases developed after firing. Thus, frit compositions without nucleating agents crystallise through a surface nucleating process and they lead to glass–ceramics with cordierite as the main phase. Occasionally, enstatite ($MgSiO_3$) appears as minor phase. In contrast, nucleating agents promote bulk crystallisation and titanium-containing compounds, such as rutile (TiO_2) or magnesium titanate ($MgTi_2O_5$) are present together with cordierite in glass–ceramics. Glazes were prepared from suspensions of borosilicate-sodium (20%) and cordierite-based frits (80%) in water. The borosilicate frit increased the coefficient of thermal expansion to match the clay support more closely.

Unlike the cordierite frits, borosilicate glass does not crystallise on firing, ensuring a good adhesion of the glaze to the clay support and minimal surface porosity of the glaze. However, the dilution of cordierite-based frits with the borosilicate frits resulted in glazes where magnesium silicates, such as enstatite ($MgSiO_3$) and forsterite (Mg_2SiO_4), were the major crystalline phases. Only the frit composition with the lowest $SiO_2/(Al_2O_3 + MgO)$ value (1.2) was capable of crystallising cordierite (2–3 µm in size) under a fast-firing cycle for tile production. In addition, this frit was the only one to give a homogeneous, nonporous, completely crystallised glaze when applied to a clay support. The authors claimed that the presence of cordierite crystals in the glaze should enhance abrasion and acid resistance, although they did not conduct any tests to confirm this statement.

Devitrification of some glass compositions in the $CaO–MgO–Al_2O_3–SiO_2$ quaternary system also leads to cordierite-based glass–ceramics [99, 100]. Nevertheless, although CaO in the quaternary system acts as a flux [101] and the required temperatures to generate the liquid phase are lower than for the $MgO–Al_2O_3–SiO_2$ ternary system, the addition of complementary fluxes is necessary to attain full development of the glaze layer. Torres and Alarcón [102] studied the effects of several additives (B_2O_3 and/or a mixture of Na_2O and K_2O in a weight ratio of 1–3 as fluxes and/or TiO_2 as nucleant), on the crystallisation behaviour of frits in the $CaO–MgO–Al_2O_3–SiO_2$ system and the morphological features of cordierite crystals formed after several heat treatments. In addition, they evaluated the viability of the studied frits as glass–ceramic glazes by fast single firing. In glasses containing TiO_2 and/or B_2O_3 as flux, α-cordierite was the main crystalline phase after firing with small amounts of anorthite ($CaAl_2Si_2O_8$) also present. In contrast, glasses containing alkaline oxides as fluxes inhibited cordierite crystallisation and led to glass–ceramics composed of anorthite. The ability of frit compositions to develop cordierite glass–ceramic glazes was evaluated after different firing schedules. Conventional fast firing at 1160 °C lead to glazes containing cordierite as the single crystalline phase. Large crystals oriented at random display well-defined hexagonal prismatic morphology, known as secondary cordierite [103]. The ability of alkaline oxides to restrain cordierite crystallisation was again highlighted by the same authors in the study of glass–ceramic glazes in the $ZnO–MgO–B_2O_3–Al_2O_3–SiO_2$ system and by Rasteiro et al. [25] in glazes in the $MgO–Al_2O_3–SiO_2$ system, where the occurrence of Na_2O and K_2O as additional flux agents promotes spinel formation as nearly the only crystalline phase as opposed to the cordierite phase [88].

In a subsequent study [104], Torres et al. followed the mechanism of crystallisation under fast-firing processing to obtain a better understanding of the entire crystallisation process from a frit consisting of 4.66 CaO, 12.01 MgO, 21.57 Al_2O_3, 55 SiO_2, 3.86 TiO_2, and 2.90 B_2O_3 (wt%). Crystallisation begins at temperatures close to 900 °C, and in glazes fired above 1000 °C α-cordierite is the only crystalline phase, developed directly from the glass without prior μ-cordierite crystallisation. Addition of B_2O_3 assisted densification by viscous flow before crystallisation, and nucleation of α-cordierite occurred on the boundaries of the original glass frit particles. The fast-firing process leads to highly crystalline glazes (69.5 wt% cordierite) with a microstructure consisting of an arrangement of well-shaped hexagonal prisms with sizes <3 µm precipitated in a residual glassy phase.

Glasses in the $CaO–MgO–Al_2O_3–SiO_2$ quaternary system are also able to devitrify anorthite by enhancing the amount of CaO and, consequently, inhibiting α-cordierite as the only crystalline phase. On the other hand, the MgO content is also critical to crystallising large amounts of α-cordierite. In this context, Torres and Alarcón [105] explored the effect of the MgO/CaO ratio on the development of cordierite-based glass–ceramic glazes, mainly with the aim of attaining the highest cordierite formation. For this purpose, they studied three frits with compositions (in wt%) 55 SiO_2, 21.5 Al_2O_3, $(16.5 - x)$ MgO, x CaO, 3.8 TiO_2 and 2.9 B_2O_3 (with $x = 6.5$, 4.6, and 2.9). After fast firing at 1100 °C, only the composition with 4.6% of CaO leads to a glass–ceramic with cordierite as the only crystalline phase. Moreover, this composition was the best at promoting cordierite formation after fast firing at 1190 °C. Higher CaO content favoured the formation of anorthite, whereas higher MgO content promoted enstatite ($MgSiO_3$) and forsterite (Mg_2SiO_4) crystallisation. However, fast firing at higher temperatures (1160 and 1190 °C) gave rise to glass–ceramics composed merely of α-cordierite (Fig. 9). The authors highlighted that with a higher amount

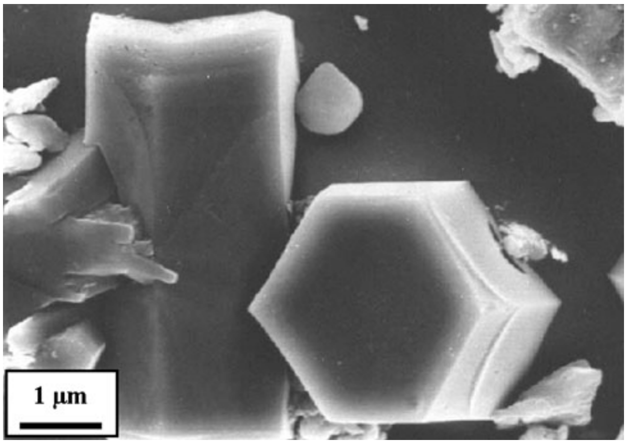

Fig. 9 α-cordierite hexagonal prisms in a glass with composition 4.66 CaO, 12.01 MgO, 21.57 Al_2O_3, 55 SiO_2, 3.86 TiO_2 and 2.90 B_2O_3 (wt%) heated at 1160 °C for 5 min [105]

of cordierite in the glazes, the best shaped crystals and the highest microhardness (ranged in the 562–710 kg/mm^2 interval) were obtained in the final glass–ceramic glaze.

As already mentioned, glass–ceramic glazes in the CaO–MgO–Al_2O_3–SiO_2 system commonly include TiO_2 as a nucleating agent to control the glass/crystal ratio and the crystal size and shape. However, as discussed above, TiO_2 is known to cause opacity and yellowing in the glaze. To avoid these undesirable aesthetic effects, an alternative to the use of nucleating agents is to introduce crystallisation seeds in the glass, inducing development of particles with the same structure as the crystalline phase. This will decrease the nucleation activation energy, as the introduction of heterogeneities leads to preferential nucleation positions at low-energy epitaxial interfaces, thereby increasing the frequency of nucleation. In this context, Martínez et al. [106] developed seeds of α-cordierite phase by the sol–gel process, which were subsequently introduced (3 wt%) together with a commercial gloss transparent frit in a glaze composition. The study found that the gels were able to give rise to cordierite crystallisation, but saphirine ($4MgO{\cdot}4Al_2O_3{\cdot}2SiO_2$) was also present as major phase and cerianite (CeO_2), introduced in the gel composition as a nucleating agent, remained as a minor phase. Unfortunately, the authors did not give additional details on the degree of crystallisation of cordierite or the microstructure of this ceramic glaze.

Currently, one of the technical performance characteristics demanded in ceramic tile is the non-slip effect (friction coefficient), as new regulations on materials use in public and high traffic pavement have recently been introduced [107]. With this in mind, Rincón et al. have explored the synthesis of glass–ceramic glazes in the MAS and CMAS systems and they have shown that cordierite crystals could improve the properties of friction on the glaze surface, thus obtaining useful anti-slip glazes.

Inosilicates ((SiO_3^{2-}) single chains)

Diopside ($CaMgSi_2O_6$) glazes

As has been mentioned, ceramic tile is made up of two components: a stoneware or porcelain support and a glaze covering. Although the properties of the ceramic tile depend on the properties of each of the components, some mechanical properties, such as wear resistance and Vickers hardness are strongly influenced by the specific properties of the glassy layer [108].

In the 1990s, there was a rising demand for ceramic tiles with improved technical properties, including high surface hardness and resistance to wear by abrasion, as well as good chemical resistance. It was well known that the mechanical properties of glass–ceramics are better than the corresponding to the original glass. Thus, several researchers thought that the development of glass–ceramic glazes could be an appropriate approach to enhanced mechanical properties in ceramic tiles. Indeed, in an earlier paper, Atkinson et al. [109] have indicated that the stresses generated by the devitrified crystals, their size and the mean free path were responsible of the reinforcement of the glassy matrix. However, the main handicap was the need to adapt glass devitrification to the fast-firing industrial process used in the manufacture of ceramic tiles.

In the late 1980s came the development of the material known as 'Silceram', a glass–ceramic with composition in the CaO–MgO–Al_2O_3–SiO_2 quaternary system [110, 111] and made up of pyroxene (diopside) as main crystalline phase formed in the 900–1000 °C temperature interval. Silceram was endowed with high chemical and mechanical properties and hence, pyroxene appeared to be very attractive crystalline phase for further development in glazes.

Founded on the aforementioned research conducted for Silceram development, Baldi et al. [112] carried out the first study to assess the feasibility of devitrifying a pyroxene phase in glass–ceramic glazes and studied the effects of common nucleating agents TiO_2, ZrO_2 and P_2O_5 (0–10 wt%) on the crystallisation process of a frit consisting of 50 SiO_2, 25 CaO and 25 MgO (wt%) and its potential for adaptation to a fast-firing cycle. Although frit composition was within the forsterite stability field of the ternary CaO–MgO–SiO_2 system, all frits devitrified diopside ($MgCaSi_2O_6$) regardless of the inclusion of a nucleating agent. However, TiO_2 acted as nucleating agent by reducing both crystallisation temperature and activation energy and led to a dense microstructure with very fine grain size (<0.5 μm) of diopside, whereas ZrO_2 and P_2O_5 delayed the crystallisation process. These glass–ceramic glazes showed great crystallinity and appeared compatible with the clay support, and were considered appropriate for use as tile glazes. Years later, Romero et al. [113] investigated the effect of iron oxide on diopside crystallisation in glass–ceramic glazes and highlighted that like ZrO_2 and P_2O_5, Fe_2O_3 did not promote the growth of diopside phase.

Based on the previous investigations, Torres and Alarcón [112, 114] explored the effect of some additives, fluxes and nucleating agents, on the crystallisation of diopside in glasses in the MgO–CaO–Al_2O_3–SiO_2 quaternary system. To ensure the crystallisation of pyroxene as the only crystalline phase, the addition of a mixture of K_2O and Na_2O was required, which led to well-formed pyroxene prismatic crystals around 2 μm size (Fig. 10a). The role of alkaline oxides was to not only lower the viscosity and facilitate sintering but also structural, taking part in the formation of solid solutions with the pyroxene structure. The Vickers microhardness of glazed tile yielded the value of 620 MPa,

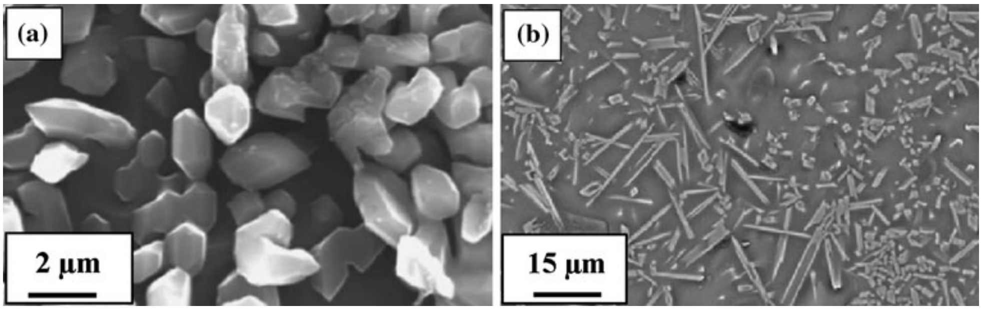

Fig. 10 **a** FESEM micrograph showing pyroxene prismatic crystals in a glaze with composition 57.68 SiO_2, 10.58 Al_2O_3, 9.62 MgO, 15.39 CaO, 2.88 B_2O_3, 2.88 K_2O and 0.96 Na_2O (wt%) fast heated at 1190 °C for 5 min [108] and **b** Backscattered SEM-micrograph showing columnar diopside in a glaze with composition 54.5 SiO_2, 10.1 Al_2O_3, 4.0 MgO, 17.4 CaO, 2.3 K_2O and 1.8 Na_2O (wt%) fired at 1215 °C according to a fast-firing cycle [118]

which is higher than that for conventional glazes, usually lower than 560 MPa. High microhardness owing to diopside crystallisation was also reported by Yekta et al. [115] studying the CaO–MgO–SiO_2–Al_2O_3–ZrO_2 system to develop tile glazes with improved surface hardness and glossiness. The investigation showed that although gradual addition of CaO and MgO to a base glaze increased the crystallinity of diopside, it also resulted in an unfired glaze surface. Addition of 2.5 wt% of ZnO slightly reduced the crystallinity, causing an improvement in the smoothness of the glaze surface. The authors reported Vickers microhardnesses up to 732 MPa. The gradual reduction of diopside crystallisation with ZnO content was corroborated by Pekkan and Karasu [116] in the study of frit-based glaze compositions belonging to the K_2O–MgO–CaO–ZnO–Al_2O_3–B_2O_3–SiO_2 glass–ceramic system.

A critical factor in the development of diopside glass–ceramic glazes is the molar ratio of magnesia to lime. Fröberg et al. [117–119] showed the influence of firing cycle on the crystalline phases developed in fast-fired raw (un-fritted) glazes in the CaO–MgO–Al_2O_3–SiO_2 system and pointed out that when MgO:CaO > 0.2 the glaze was composed of columnar diopside crystals (2–5 μm) (Fig. 10b); MgO:CaO ≈ 0.2 resulted in the combined crystallisation of diopside and wollastonite ($CaSiO_3$); MgO:CaO < 0.2 gave only wollastonite, and MgO:CaO $= 0$ resulted in pseudowollastonite. The amount of quartz also seemed to influence the precipitation of wollastonite and diopside. If the quartz content was low, only diopside was observed, thus suggesting that all the quartz available is consumed in diopside formation. Similarly, diopside formation was also found to be sensitive to both glaze composition and firing time in raw glazes in the R_2O–RO–Al_2O_3–SiO_2 system and diopside plate-like crystals (2–10 μm long) were identified if magnesia content was higher than 2 wt%. The authors highlighted the high chemical resistance of diopside glazes in several acidic and alkaline aqueous solutions. Diopside crystals showed no signs of attack after immersion in HCl, and analysis of the hydrochloric solution after the test suggested that diopside had not corroded.

Recently, Reinosa et al. [120] reported the development of nanostructured glass–ceramic glazes produced by a spinodal decomposition process in which a pyroxene nanocrystalline phase was homogeneously distributed along the whole glaze. The nanosize of the crystalline phase, <100 nm, is quite below visible wavelengths, and subsequently it results in a transparent glossy glaze.

Wollastonite ($CaSiO_3$) glazes

Base glasses of the CaO–Al_2O_3–SiO_2 system are especially appropriate for producing glass–ceramics according to the mechanism of controlled surface crystallisation. Wollastonite glass–ceramics exhibit special optical effects and other favourable properties, which have propitiated that these materials are produced on a large scale and used as cladding in the building industry [3]. The most significant wollastonite glass–ceramics for architectural applications are marketed under the brand names Neoparies™ (Nippon Electric Glass) and Cryston® (Asahi Glass Co.) and both are produced by a sinter-crystallisation process, in which glass grains are sintered to a dense monolithic glass by heat treatment. At approximately 950 °C, controlled surface crystallisation of β-wollastonite (CaO·SiO_2) begins at the boundary of the glass grains, and at 1000 °C, wollastonite grows in a needle-like form from the surface of the glass to the centre of the glass grain.

Sanmiguel et al. [121] undertook a devitrification study of a high calcium content frit in the CaO–MgO–SiO_2 system, which would be applied as a granular on a base glaze. Granular glazes are widely used materials in the ceramic floor and wall tile sector as a complement to the base glazes, so that they remain on the tile surface after firing; thus, granular glaze is the first constituent to undergo wear upon use. Wollastonite crystallisation in the granular glaze occurs through a heterogeneous nucleation process at the interfaces. The activation energy associated with wollastonite crystallisation from the interface granular-base glaze (about 70 kJ/mol) is lower than that from the air-granular interface (about 110 kJ/mol). Hence, in the firing process, wollastonite crystallisation initiates at the granular-glaze interface and subsequently at the granular-air interface, advancing in all directions towards the interior of the granular particle.

Sorlí et al. [76] found wollastonite crystallisation in a ceramic glaze from a frit in the ZnO–CaO–SiO_2 system with 5 wt% K_2O as flux and equilibrium CaO–ZnO. Wollastonite devitrifies as acicular crystals of 2–4 μm dimensions in an anastomosed acicular microstructure and leads to glazes with lower scratch resistance and greater microhardness, which results in higher brittleness indices. However, ZnO content in the glaze composition should be optimised, as it has been found that high levels of ZnO may lead to the dissolution of wollastonite into the residual glass phase [115, 116]. Benet et al. [122] also explored wollastonite crystallisation in a frit of the ZnO–CaO–SiO_2 system. A glaze composition containing 90 wt% granular (<500 μm), 10 wt% bentonite and 6 wt% moisture was applied to porcelain stoneware bodies by a double pressing process. After a fast-firing process, they obtained a glass–ceramic glaze composed mostly of wollastonite, possibly as result of the reaction of the silica presents in the glassy phase with bentonite.

Fröberg et al. [117, 119] studied the effect of glaze composition and firing conditions on the final phase compositions developed in raw glazes in the CaO–MgO–Al_2O_3–SiO_2 system. As was above explained (in the diopside section), the molar ratio of magnesia to lime was found to control the crystal type. Thus, wollastonite was found to be formed in compositions high in lime, but low in alumina and magnesia. Accordingly, MgO:CaO < 0.2 leads to tiny (2–5 μm) and columnar wollastonite crystals, whereas MgO:CaO $= 0$ gives hexagonal pseudowollastonite (Ø = 2–10 μm) as main crystalline phase in the glazes (Fig. 11).

However, the biggest drawback of wollastonite-based glazes is the chemical resistance, as wollastonite crystals devitrified in glazes are readily attacked by acidic or slightly alkaline water solutions [123–126]. Wollastonite and pseudowollastonite corrosion was observed mainly along the interfacial layer between the crystals and glassy phase, crystal planes and boundaries [127]. Fröberg et al. [118] attempted to shed light on the corrosion mechanisms of wollastonite and pseudowollastonite by analysing the glazed surfaces before and after immersion and analysing the immersion solutions. The authors pointed out that both tiny columnar wollastonite and pseudowollastonite crystals were easily dissolved in all but the most alkaline solution and first signs of attack could be seen after 5 min (Fig. 12). The analysis of the hydrochloric acid solution after the immersion of glazes for different periods clearly indicated increased concentrations of calcium and silicon ions. The calcium ion concentration increased at a faster rate than the silicon ion concentration for both glazes, suggesting an incongruent dissolution of the crystals. In situ pH measurements of glazes in hydrochloric acid showed increased values as a function of immersion time. However, when the glazes were immersed in ultra pure water, a minor increase in pH from roughly 7 to 7.5 was observed.

Spodumene ($LiAlSi_2O_6$) glazes

Glass–ceramics in the Li_2O–Al_2O_3–SiO_2 system are recognised for their exceptional features, such as near zero thermal expansion, high transparency and transmissibility. These properties make spodumene glass–ceramics applicable in a broad range of applications. Rincón et al. [128] explored the capabilities of commercial glass–ceramic compositions in use as glass–ceramic glazes. Among other crystalline phases, they reported the development of glazes containing prismatic crystals of spodumene

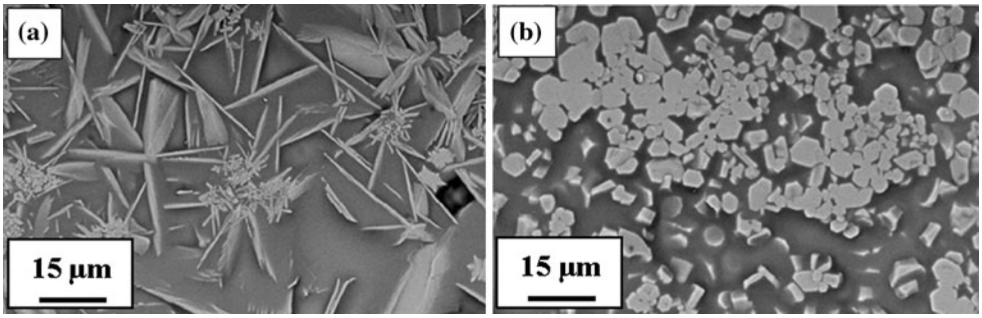

Fig. 11 Backscattered SEM-micrograph of glazes fired at 1215 °C according to a fast-firing cycle, showing **a** dendritic wollastonite in a glaze with composition 56.0 SiO_2, 17.5 Al_2O_3, 2.0 MgO, 17.5 CaO, 3.8 K_2O and 3.2 Na_2O (wt%) and **b** hexagonal pseudowollastonite crystals in a glaze with composition 45.4 SiO_2, 17.7 Al_2O_3, 0.2 MgO, 30.0 CaO, 3.8 K_2O and 3.2 Na_2O (wt%) [118]

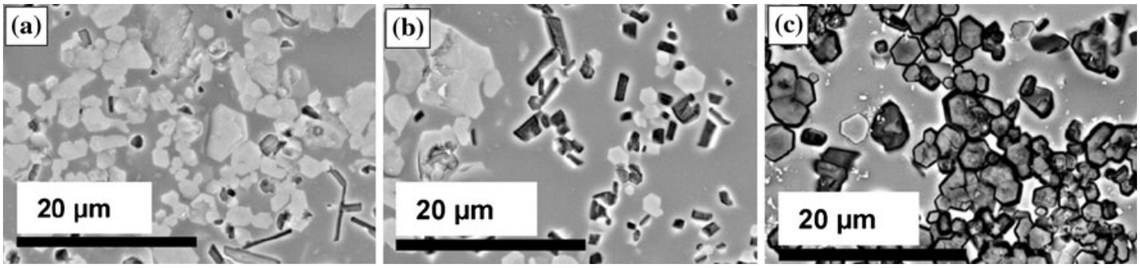

Fig. 12 SEM-micrographs of corrosion of a pseudowollastonite glaze with composition 45.4 SiO_2, 17.7 Al_2O_3, 0.2 MgO, 30.0 CaO, 3.8 K_2O and 3.2 Na_2O (wt%) after immersion in hydrochloric acid for **a** 15 min; **b** 30 min; and **c** 2 h [118]

($Li_2O{\cdot}Al_2O_3{\cdot}4SiO_2$) from a commercial glass–ceramic composition and leucite ($K_2O{\cdot}Al_2O_3{\cdot}4SiO_2$) whiskers (1–2 μm length) in glazes from frits in the Li_2O–K_2O–Al_2O_3–SiO_2 system. In all cases, the glazes showed thermal expansion coefficients matching the ceramic substrate.

Leonelli et al. [129] reported the possibility of crystallising spodumene in glazes with compositions derived from industrial formulations belonging to the classical Li_2O–Al_2O_3–SiO_2 glass–ceramic system. The crystallisation study revealed that the development of β-spodumene is mainly controlled by the percentage of lithium, aluminium and silica in the glaze composition and is not influenced by the chemical composition of the residual glass. In the studied glazes, β-spodumene crystals grow as strongly interlocked crystals of about 1–5 μm size.

Glass–ceramic glazes with spodumene as the main crystalline phase have also been prepared by Martínez et al. [106] from a xerogel of composition 60–65 SiO_2, 20–25 Al_2O_3, 2–10 Li_2O, 3–6 Ce_2O_3 and 0–5 B_2O_3 (wt%) using sol–gel technology. The xerogel (3 wt%) added to a commercial frit for porcelain stoneware acted to seed the crystallisation of spodumene crystals homogeneously dispersed in the glaze.

Phylosilicates ($(Si_2O_5)^{2-}$, $(AlSi_3O_{10})^{5-}$ or $(Al_2Si_2O_{10})^{6-}$ sheets)

Biotite ($K(Mg,Fe^{2+})3(Al,Fe^{3+})_3O_{10}(OH,F)_2$) *glazes*

Romero et al. [130] reported the crystallisation of biotite in glass–ceramic glazes from a high fusibility glassy frit containing 10 wt% fluorine. The development of biotite crystals with hexagonal and rectangular habits is promoted by the occurrence of iron oxide in the glaze composition. Thus, increasing iron content up to 16.01 wt% leads to spatial orientation of biotite crystals with respect to the glaze surface. The development of preferential crystal orientation in the mica glass–ceramic glaze, together with substantial interlocking of crystals resulted in the improvement of superficial mechanical properties.

Tectosilicates (SiO_2, $(AlSi_3O_8)^{1-}$ or $(Al_2Si_2O_8)^{2-}$ three-dimensional framework)

Silica polymorph (SiO_2) *glazes*

The crystallisation of cristobalite or tridymite in glazes might be of interest for development of transparent glass–ceramic glazes. The transparency or opacity of a polycrystalline material depends on the internal refractions that occur within the material [131]. Therefore, to achieve a transparent effect in these conditions, it is necessary that the different phases exhibit similar refractive indices. Assuming that the refractive index of glass is 1.5, to obtain a transparent glass–ceramic glaze the presence of crystalline phases with similar refractive index is required [122]. Tridymite and cristobalite, both silica polymorphs, are suitable.

The ZnO–CaO–SiO_2 system shows that tridymite and/or cristobalite could be achieved in glass compositions with high-silica content and low CaO and ZnO, thus preventing the formation of silicates of calcium and zinc as wollastonite ($CaSiO_3$) and willemite (Zn_2SiO_4). Low percentages of Al_2O_3 are also necessary, as this oxide inhibits devitrification of silica to tridymite and cristobalite, favouring the formation of mullite ($3Al_2O_3{\cdot}2SiO_2$). However, tridymite or cristobalite devitrification is not facile following a fast-firing process. Sanmiguel et al. [121] studied the devitrification of a commercial frit with a high calcium content, reporting that cristobalite crystals develop through a homogeneous nucleation mechanism with activation energies linearly increasing with particle size from 400 kJ/mol for the size fraction of 100–200 μm up to 510 kJ/mol for 700–800 μm. These high values of activation energy suggest that cristobalite formation was kinetically hindered in a fast-firing process, which will favour the crystallisation of phases with lower activation energy. In these cases, the glaze cristobalisation only occurs for long holding times at the firing temperature.

Martínez et al. [106] developed seeds of α-cristobalite phase by the sol–gel process, which were subsequently introduced (3 wt%) together with a commercial gloss frit in a glaze composition. Through this processing method, the authors have developed by a single-firing industrial process, highly crystallised transparent glass–ceramic glazes, in which cristobalite appears as the only crystalline phase.

Anorthite ($CaAl_2Si_2O_8$) glazes

Anorthite ($CaO \cdot Al_2O_3 \cdot 2SiO_2$) is one of the main crystalline phases developed in slag sitals (glass–ceramics produced from industrial slags). Anorthite type glass–ceramics are characterised by high mechanical strength and good chemical durability [117]. Glass compositions that lay in the primary crystallisation field of anorthite devitrify easily, but they are not readily internally nucleated. The materials do, however, form good powder processed (fritted) glass–ceramics [3]. Thus, frits with such compositions should lead to anorthite-based glazes with intermediate coefficients of thermal expansion.

Fortanet et al. [132] studied the crystallisation of anorthite phase in the $CaO–Al_2O_3–SiO_2$ system, in order to obtain glass–ceramic glazes with improved surface frictional properties, specifically non-slippery glazes. In this way, they developed frits composed of 40–50 SiO_2, 25–40 Al_2O_3 and 10–20 CaO (wt%), which were applied over two different glass–ceramic glazes for porcelain stoneware tiles. After fast firing, the anorthite glazes show superior Mohs hardness and Vickers microhardness and in addition, the glazes exhibit a dynamic friction coefficient (Tortus method) in the 0.89–0.91 range, greater than the value of 0.75 recommended by the Transport Road Research Laboratory.

Reinosa et al. [120] evaluated the thermal behaviour of a glaze used for transparent and glossy glazes based on the $SiO_2–CaO–ZnO–Al_2O_3$ system. A glaze with 59 SiO_2, 3 B_2O_3, 9 Al_2O_3, 13 CaO, 11 ZnO and 4 K_2O (wt%) was deposited on a green clay-based ceramic stoneware support. Anorthite appears in the glaze after firing at 950 °C after the short time of 1 min, as a result of the reaction between the metakaolin from the ceramic support and the glassy matrix during the earliest stage of the sintering step. Longer hold times at the firing temperature led to the development of diopside phase together with anorthite.

In tile manufacturing, α-Al_2O_3 is frequently used as a matting agent in glazes [133–135]. Bou et al. [87] examined the effect of different types of alumina on the technical and aesthetic properties of glazes formulated from a transparent frit composed of 58 SiO_2, 3 B_2O_3, 6 Al_2O_3, 12 CaO, 3 MgO, 11 ZnO and 5 K_2O (wt%). The authors reported that upon firing, anorthite formation is caused by Al_2O_3 dissolution in the glassy phase surrounding the alumina particles, where the presence of CaO and SiO_2 from the glassy phase favours anorthite crystallisation. The effectiveness of alumina particles in promoting anorthite formation in glazes had been also reported by Rasteiro et al. [25] in a study on the influence of some additives on properties of commercial glass–ceramic glazes.

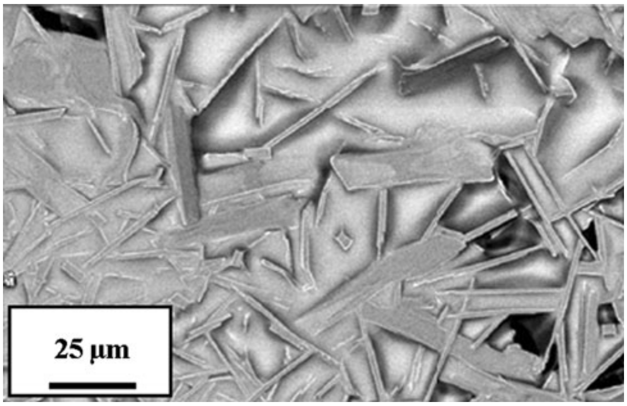

Fig. 13 Backscattered SEM-micrograph showing flake-like anorthite crystals in a glaze with composition 49.5 SiO_2, 25.0 Al_2O_3, 4.0 MgO, 17.5 CaO, 2.2 K_2O and 1.8 Na_2O (wt%) fired at 1215 °C according to a fast-firing cycle [118]

Anorthite in glass–ceramic glazes usually crystallises as flake-like crystals (Fig. 13) and it has been found that anorthite exhibits excellent durability in alkaline and acidic solutions [136–138]. Fröberg et al. [118] analysed the chemical resistance of anorthite glazes in water solutions and they found no signs of attack on the flake-like anorthite in any of the acidic or alkaline test solutions. Only minor changes were observed in the ion concentrations of the hydrochloric acid solution. It was assumed that as anorthite formed in glazes with high corundum contents, the glassy phase was also high in alumina, leading to increased surface durability.

Oxide-based glass–ceramic glazes

Anatase–rutile (TiO_2) glazes

Traditionally, industrial glazes for ceramic tiles use zircon or zirconia as opacity agents for coatings, the former being much more common due its lower cost. However, the price of raw materials containing zircon is continually increasing, spurring the search for new compositions of non-bearing zircon frits also leading to glossy opaque white glazes.

One useful candidate for zircon replacement is titanium dioxide, which can crystallise in different polymorphs: rutile and anatase (tetragonal) as well as brookite (orthorhombic). Rutile is the only stable phase, while the two metastable phases, anatase and brookite, irreversibly transform to rutile on heating. The high refractive indices for rutile (2.76) and anatase (2.52) make titania polymorphs excellent candidates to zircon replacement in glazes. Titanium dioxide in the form of anatase is a bright white powder with high opacity and excellent covering power, chemical and physical resistance. These excellent optical characteristics, coupled with its high refractive index, make it a valuable pigment and opacifier [139].

Titanium oxide has been widely used in the formulation of porcelain glazes and metal enamels [140–142], where TiO_2 crystallites created during firing yield opacity. However, in such enamels, TiO_2 generates non-white coatings. Thus, the colour varied from blue to yellow depending of the rutile/anatase ratio in the fired enamel. A yellow colour was associated with large rutile particles, whereas a blue colour was attributed to smaller rounded anatase particles.

In half of the 1970s, TiO_2 was commonly used in large amounts (15–20 wt%) to opacify thin layers of metal enamels maturing in the range 750–850 °C. However, the few examples of white TiO_2-opacified glazes reported in the literature were not suitable for industrial production. When TiO_2 was used to opacify ceramic glazes maturing at higher temperatures with a lower coefficient of thermal expansion, yellowish glaze surfaces were obtained. Biffi et al. [143] conducted research aimed at developing opaque white ceramic glazes from a base frit with TiO_2 content in the 4.5–7.5 wt% range. Satisfactory white glossy glazes were obtained with reflectivity values very similar to those obtained from zircon opacified glazes. The study reported that the opacity was not due to rutile or anatase particles, but the presence of a calcium titanium silicate, $CaTiSiO_5$ (sphene), crystallised from the melt. Sphene (refractive index of 1.9) developed during heating is wholly dissolved at firing temperature and devitrifies again during cooling. By comparing refractive indexes, densities and molecular weights of $CaTiSiO_5$ with TiO_2 (both as anatase and rutile), the authors revealed that the amount of TiO_2 required as $CaTiSiO_5$ to opacify the glaze should be equal to half the anatase or rutile used to that effect. Indeed, the optimum TiO_2 concentration in glazes opacified by $CaTiSiO_5$ is about 5–5.5 wt% compared to the 9–10 wt% required when opacification is produced by TiO_2 particles of the same size. Wear resistance and chemical resistance to acids and bases were found to be excellent in all cases except when TiO_2 contents were lower than 4% wt.

The evolution of colour in glazes containing titanium dioxide was studied many years later by Moreno et al. [144] in a series of compositions prepared with different proportions of anatase (3–15 wt%) added to a basic formula consists of a single-firing frit, which resulted in transparent glazes, and dolomite (0–10 wt%). The addition of anatase in small percentages (3%), lead to a noticeable increase in the bluish colour without modifying the glaze transparency and gloss. This is probably due to the separation of immiscible liquid phases that occur as result of the total dissolution of anatase during firing, while the devitrification of crystalline phases of titanium does not take place. By increasing the amount of anatase added (6–9%), the glaze showed a significant increase in opacity, while the blue colour and gloss were reduced. The increase in titanium in the liquid phase, produced by dissolution of anatase, was great enough to form sphene in combination with calcium and silicon, which significantly increased the degree of opacity and whiteness and progressively masked the bluish colour caused by phase separation. Higher percentages of anatase (15%) enlarged the amount of titanium in the glassy phase by dissolution of anatase, until an excess of titanium with respect to calcium occurred and led to rutile crystallisation. Rutile has a yellowish shade, and the yellow colour of the glaze increased with the proportion of rutile, though the opacity scarcely changed, as rutile has a high refractive index (2.76). In addition, the crystal size of rutile is larger than that of sphene, causing an increase in the roughness of the glaze and thus, a reduction in gloss.

Teixeira and Bernardin [145] reported on the use of titania polymorphs (rutile and anatase) as the main component for producing white opacity in ceramic glazes for tile coatings. Total zirconia (12% mass fraction) contained in a frit in the SiO_2–Al_2O_3–B_2O_3–CaO–K_2O–ZrO_2 system was replaced by rutile and by anatase in mass fractions of 5, 10 and 15%. The frit containing 10% anatase generated a white glaze with high coating capacity, whereas frits containing rutile resulted in yellow opacity. All glazes were composed of sphene and rutile crystals and the main difference between glazes is that the sphene phase was more developed in glazes from rutile frits. The study concluded that frit compositions based on the SiO_2–Al_2O_3–B_2O_3–CaO–K_2O–TiO_2 system are able to produce opaque white glazes, but such glazes present lower gloss than those obtained with ZrO_2 containing frits. Gloss could potentially be increased by the replacement of K_2O by Na_2O in the frit composition. However, this substitution is not feasible because Na_2O increases glaze fusibility at low temperatures.

Escardino et al. [146] reported that an alternative way to enhance glaze gloss in TiO_2 glazes is through the addition of small amounts of phosphorus pentoxide (P_2O_5) to the frit composition. Based on this work, Bou et al. [147] conducted a detailed study to establish how the addition of P_2O_5 contributes to increasing gloss in opaque whitewall tile glazes. The study was achieved using a starting frit composition consisting of 64.0 SiO_2, 4.6 Al_2O_3, 5.0 B_2O_3, 13.9 CaO, 5.9 K_2O and 6.5 TiO_2 (wt%) with gradual additions of P_2O_5 (from 0.5 to 3 wt%). The addition of 1% P_2O_5 increased glaze gloss and yielded glossy glazes with characteristics similar to those obtained in glazes from frits that contained ZrO_2. P_2O_5 favours the formation of small-size sphene crystals over other crystalline phases as wollastonite, which devitrifies in the form of large crystals that enlarge surface roughness and therefore reduce glaze gloss.

Chen and Liu [148] conducted qualitative and quantitative characterisation of sphene nucleation and crystallisation in a CaO–TiO_2–B_2O_3 bearing ceramic frit and an analogous non-borate base glass. Sphene was the first crystalline phase nucleated in the frit, with an onset crystallisation temperature of 800 °C. At 850 °C $CaTiSiO_5$ was markedly nucleated along grain boundaries though crystal sizes were variable, typically smaller than 1 μm. At 1050 °C, $CaTiSiO_5$ crystals exhibited larger size (1–3 μm) and were generally peanut shaped, being aligned into feather-like morphologies. Sphene was the main crystalline phase in the fired frit, whereas wollastonite (α-$CaSiO_3$) was developed as a minor phase in the non-borate base glass and $CaTiSiO_5$. The authors justified the relative prevalence of sphene and wollastonite phases on the basis of the CaO:TiO_2 ratio. A high CaO:TiO_2 content tends to favour α-$CaSiO_3$, whereas a lower CaO:TiO_2 ratio supports $CaTiSiO_5$ crystallisation.

In a recent study, Rodriguesa and Bernardin. [149] highlighted the importance of melting and glazing conditions on sphene and rutile crystallisation and hence, on white opacity in ceramic tile coatings. An anatase frit (10 wt% TiO_2) was melted at 1480 °C for 60 min (F1 frit) and 90 min (F2) and 1530 °C for 60 min (F3) and 90 min (F4). Green glazed tiles were fired at 900, 1000, 1100, and 1190 °C for 40 min. Sphene was one of the main phases, together with other major and minor crystalline phases. At 1100 °C for 40 min, β-quartz appeared as the major phase with rutile as a minor phase, whereas rutile was the major phase in frit F2 and β-quartz was not detected. In frit F3 rutile occurred as the major phase with quartz as a minor phase, but rutile was not formed in F4. Only quartz and albite were observed as minor phases. At 1190 °C for 40 min there was a decrease in the crystallinity of all glazes, with the main phases identified in frit F1 (1530 °C/60 min) and F3 (1480 °C/60 min) being sphene and rutile, with a large glassy phase. For F2 (1530 °C/90 min) only sphene was identified and there was an increase in the glassy phase. Finally, for the F4 frit (1480 °C/90 min), the main phases formed were also sphene and β-quartz, this being the glaze with the smallest glassy phase.

Atkinson et al. [150] reported the influence of additions (10 wt%) of rutile and anatase on the structure of a base oxide glaze consisting of 59.4 SiO_2, 15.0 Al_2O_3, 12.0 RO, 8.6 R_2O and 5.0 ZnO (wt%). The crystalline phases present in the standard glaze are quartz and plagioclase, and rutile was also identified in both glazes with 10% TiO_2 addition. IR indicated that the glazes were in general highly disordered and ^{29}Si MAS NMR data clearly showed that upon addition of the opacifiers, the glaze became much more highly disordered.

Spinel ($MgAl_2O_4$) glazes

Glass–ceramics based on spinel compositions ranging from gahnite (ZnO·Al_2O_3) to spinel (MgO·Al_2O_3) were obtained by controlled crystallisation of glasses in the ZnO–MgO–Al_2O_3–SiO_2 quaternary system [151, 152]. The presence of TiO_2 as nucleating agent favours the nucleation of crystal phases by fine-scale glass-in-glass phase separation leading to a fine- or ultrafine-grained glass–ceramic. The microstructure of spinel glass–ceramics provides special properties. Given the small dimensions of spinel crystals and their fine distribution in the glass matrix, the glass–ceramics are transparent in the visible spectrum and exhibit minimal scattering [3].

Considering the intrinsic physical properties of the spinel crystalline phase, Torres et al. [88] attempted to develop spinel-based glass–ceramic glazes. They tested the viability of a frit composed of 53 SiO_2, 29 Al_2O_3, 6 B_2O_3, 9 MgO and 3 ZnO (wt%) for producing spinel-based glass–ceramic glazes and reported the effects of additional flux (B_2O_3, Na_2O and K_2O) and nucleating agents (TiO_2) on the crystallisation path and microstructural features of the final glaze. This study revealed that frits containing a combination of Na_2O and K_2O as flux developed spinel as the main and nearly singular crystalline phase, whereas spinel was present in lower amounts when alkaline oxides were absent from the glaze composition. Spinel crystallisation was preceded by a highly uniform phase separation into ZnO-rich and Al_2O_3-rich globular areas (Fig. 14a), from which the nucleation and growth of small well-shaped octahedral spinel crystals occurs (Fig. 14b). The lower crystallisation of spinel from the reference frit composition without additional fluxing agents can be understood because the nucleation of spinel in the glass is not as effective because the phase separation is less extended. The degree of spinel crystallisation in the final glass–ceramic glazes was around 20 wt%, which is significant enough to have a key role in the final mechanical properties of the glass–ceramic glaze and consequently in the ceramic tile products.

Franklinite ($ZnFe_2O_4$) glazes

Franklinite-based (ZnO·Fe_2O_3) glazes were reported by Romero et al. [113] in a study of the effect of iron content on crystallisation of glass–ceramic glazes of composition 56–61 SiO_2, 7–12 Al_2O_3, 7–14 CaO, 3–5 Na_2O, 1–12 ZnO and 0–16 Fe_2O_3 (wt%). The authors highlighted that the amount, size and morphology of franklinite phase is strongly influenced by the iron content in the glaze and that

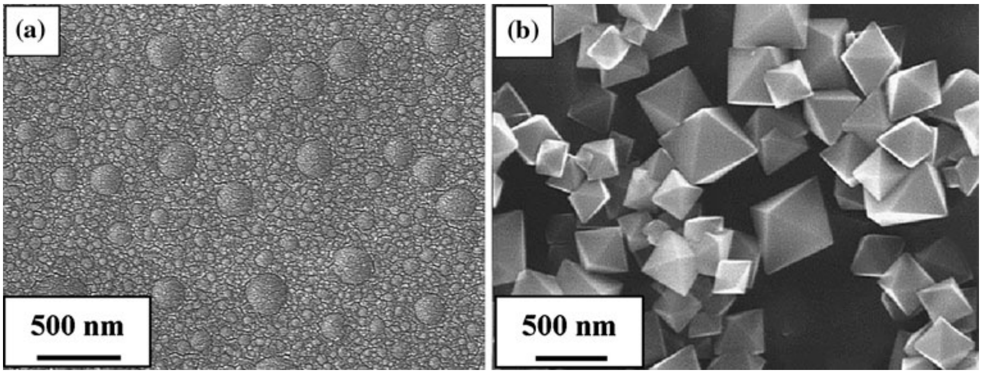

Fig. 14 SEM-micrographs in a glaze of composition 51.0 SiO_2, 24.0 Al_2O_3, 8.7 MgO, 2.9 ZnO, 8.7 B_2O_3, 2.9 K_2O and 1.0 Na_2O (wt%) showing **a** a extended phase separation after firing at 800 °C for 5 min and **b** spinel crystals formed after heating at 1100 °C for 2 h [88]

an iron content lower than 15 wt% leads to glazes with rounded franklinite crystals as the main crystalline phase, which decrease in size with increasing iron content.

Functional glass–ceramic glazes

The enhancement of quality of life in housing, areas of social activity and work zones spurs the development of new building materials with environment-improving functions. In this sense, glazed ceramic tile has also evolved to meet social demand and thus, the glaze is no longer a material whose main tasks are to provide waterproofing and aesthetics. Indeed, glazes have come to provide functionality to the ceramic tile. Recently, the glass–ceramic glaze has come to interact with the environment and it has become a living element with a specific role to improve quality of life.

Below is a brief description of glass–ceramic glazes with specific functions, such as photoluminescent, photocatalytic or antibacterial glazes.

Glazes with photocatalytic activity

Wastewater is ‘used water’ produced daily by residents and businesses activities. The goal of sewage treatment is to remove organic matter and other pollutants from wastewater. One of the most advanced techniques in the treatment of water polluted with organic products are the advanced oxidation processes (AOPs), which are defined as near ambient temperature and pressure water treatment processes which involve the generation of hydroxyl radicals in sufficient quantity to effect water purification [153]. The hydroxyl radical (·OH) is a powerful, non-selective chemical oxidant, which acts very rapidly with most organic compounds. The advantage of AOPs is based on the potential for eliminating organic products, such as pesticides and organic and biocide colourants, which cannot be treated by other conventional techniques due to their high chemical stability and low biodegradability [154]. Among the AOPs, photocatalytic oxidation is based on the photo-excitation of a semiconductor in the near-UV spectrum. Under near-UV irradiation a suitable semiconductor material may be excited by photons possessing energies of sufficient magnitude to produce conduction band electrons (e^-) and valence band holes (h^+). These charge carriers are able to induce reduction or oxidation, respectively.

Heterogeneous photocatalysis in the presence of semiconductors is a promising technology which decomposes and mineralises organic contaminants in water by the generation of radicals (·OH, $\cdot O_2^-$) under irradiation [155]. The photodegradation process is based on the formation of a suspension of anatase in the wastewater and after a certain retention time, the photocatalyst is removed by decanting and the water is filtered. Titanium dioxide (anatase) has an energy band-gap of 3.2 eV and can be activated by UV illumination. Anatase is the most widely used photocatalyst agent in wastewater treatments because of its high photocatalytic activity, non-toxicity and durability [156]. Moreover, anatase is a cheap, readily available material and the photogenerated holes are highly oxidising. In addition, anatase is capable of oxidation of a wide range of organic compounds into harmless compounds such as CO_2 and H_2O [157]. However, heterogeneous photocatalysis requires working in a discontinuous operating regime, and leads to high processing costs because of photocatalyst particles have to be separated by filtration, coagulation, flocculation or centrifugation to separate the solution and recycle the catalyst. One way to avoid the separation step could be the use of the photocatalyst agent not as free particles, but as a devitrified crystalline phase in the glaze of ceramic tiles that cover the walls of wastewater treatment tanks. Glazes with photocatalytic activity provide new functionalities to ceramics tiles in both passive air purification and wastewater treatment. In addition to anatase, other ceramic semiconductors with adequate energy band-gap could be Fe_2O_3 (2.2 eV), ZnO (3.2 eV) or SnO_2 (3.8 eV).

Meseguer et al. [158] studied the photocatalytic ability of the three types of glazes used in ceramic tile production: a double-firing glaze for third fire (6% PbO), a fast-firing glaze for porous wall tile (10% ZnO and 4.5% ZrO_2) and a fast-firing glaze for non-porous porcelain stoneware tile (10% ZnO). The photocatalytic activity was tested in both powdered fired frits and glazed ceramic tiles. The substrates used were two compounds that are difficult to aerobic degradation using oxidising procedures: ferulic acid (*trans*-4-hydroxy-3-methoxy), a wastewater contaminant in the food industry, and Orange II ($C_{16}H_{11}N_2SO_4Na$), an azo dye used in the textile industry, which provides serious challenges in water reuse.

The photocatalytic activities of the glazes were compared with anatase powder. A double-fired frit with Pb did not show catalytic activity, in either powder fired frit or glazed tile. The monoporosa and porcelain powder fired frits showed photocatalytic activity for ferulic acid, but with long half-life time (5 h) compared with the anatase powder (2 h). From this perspective, the powdered glaze does not offer an advantage over the photocatalytic oxides. However, glazed tiles retained their photocatalytic activities with very similar half-life periods to anatase powders. In this case, the use of glazed tiles in a purification reactor would allow continuous operation, avoiding the loading of the photocatalytic oxide and the subsequent separation step. On the other hand, the use of these glazed ceramic on facades or internal walls will allow the self-purification of indoor or outdoor environments.

Ruiz et al. [159] explored the possibility of using different types of ceramic glazes composed of several crystalline phases as alternatives to anatase powder in photocatalytic treatment and cleaning processes. Glazes were developed from different frits, which devitrified the desired phases. In order to study the influence of zircon crystallisation on photocatalytic activity, several glazes were prepared from mixtures of different quantities of a standard transparent frit and a frit with a 12.5 wt% ZrO_2 content. In the study of photocatalytic degradation, the degradability of Orange II was only detected in glazes made up of anorthite ($CaAl_2Si_2O_8$), zircon (Zr_2SiO_4) and cassiterite (SnO_2). The best results were observed in zircon glazes, where the photocatalytic activity of the base glaze improved by 33%. Glazes devitrifying cassiterite and anorthite exhibited smaller improvements, on the order of 12%.

All of the studied zircon-based compositions showed a photochemical activity far from that of anatase, though those with greater ZrO_2 content exhibited half-life periods shorter than the compositions with smaller ZrO_2 content. Although the band-gap energy was 3.65 eV in all cases, the half-life periods decreased when the ZrO_2 content in the frit increased. Although the band-gap energy (E_g) values in the glazes need to be low, this condition is necessary but not sufficient to develop glazes with photocatalytic activity. The decrease in the half-life period at constant band-gap energy indicates the existence of other variables that also affect the photochemical degradation. The authors pointed out that the evolution of the microstructure plays an important role in the photocatalytic properties. ZrO_2-based glazes are composed of acicular zircon crystals that decrease in size with increased concentration (e.g. the acicular crystal length is 2 μm in the sample with 2.5% ZrO_2, and this decreases progressively to 0.8 μm in the more concentrated sample). In addition, the concentration of acicular crystals increases with the nominal quantity of ZrO_2 in the glaze composition. The greater quantity and smaller size of Zr_2SiO_4 crystals explain the improved photocatalytic activity with the increase in the nominal quantity of ZrO_2. In short, the effect of crystal concentration and morphology is more important than the band-gap energy values.

The manufacture of anatase glazes in ceramic tiles is still limited because of the phase transition of TiO_2 from anatase to rutile. Currently, photocatalytic tiles are prepared by spraying TiO_2-based membranes on previously fired tiles and subsequent heat treatment at relatively low temperature, which consequently leads to poor wear resistance and short work time. Thus, the development of a method to prepare effective, durable and high-temperature stable TiO_2-based photocatalytic ceramic is of significance. Zeng et al. [160] have developed a novel method to prepare double-firing photocatalytic ceramics tiles with a low-temperature glaze (800 °C) based on modified TiO_2. Si-, P- and Zr-modified TiO_2 nanopowders (with a molar ratio of Ti/Si/P/Zr of 1:0.2:0.14:0.19) synthesised through sol–gel and hydrothermal methods. Photocatalytic ceramics tiles were prepared by doping the modified TiO_2 in the glaze. The photocatalytic activities of the samples were evaluated by the decomposition of Orange II. Experimental results showed that Si, P and Zr modification could effectively improve the thermal stability of anatase. The ceramics based on modified TiO_2 exhibited high photocatalytic activity under light irradiation. After firing at 800 °C, the grain size of modified TiO_2 particles was about 20 nm, which is lower than the critical anatase crystalline size to transform to rutile. Si, P, and Zr modification can effectively prevent TiO_2 grains from interacting with the glaze, limiting grain growth and inhibiting the transition from anatase phase to rutile. With modified TiO_2, glazes showed considerable photocatalytic activity and the decomposition of Orange II reached nearly 80% in 3.5 h.

Glazes exhibiting antibacterial and antifungal functions

Another functionality of ceramic tile that has sparked great interest in recent years is the development of antibacterial glazed tiles, which inhibit the growth of germs and kill common types of bacteria. Qing et al. [161] investigated the development of an infrared radiant glaze and its antibacterial and antifungal activity. Infrared radiant powder was synthesised by conventional ceramic processing techniques from Fe_2O_3, MnO_2, CuO, Co_2O_3 and kaolin. The infrared radiant powder was mixed with a base frit for fast firing. The glaze without infrared radiant powder had a low infrared emissivity (0.74). With increasing infrared radiant powder content, the infrared emissivity tended to increase and the authors reported that the optimum content of infrared radiant powder in the glaze was 5%. The glaze with 3% infrared radiant powder was mainly amorphous and contained a small amount of α-quartz. The glaze with 8% of infrared radiant powder was composed of a cubic spinel s.s. of transitional metal oxides and α-quartz. The antibacterial activity of the glaze reached 91–100% when *Escherichia coli*, *Staphylocaccus aureus* and *Bacillus subtilis* were used as model bacteria. The antifungal activity of the glaze exceeded 95% when *Penicillum citrinum* was used a model fungus.

The antimicrobial activities of porcelain glazes with antimicrobial agents derived from montmorillonite intercalated with a Ag chelate ($Ag + (TBZ)_2$) were explored by Yoshida et al. [162]. In order to improve the antimicrobial activity after high-temperature firing, the co-doping effect of Al and Zr into the interlayer spaces of montmorillonite was also examined. The Ag contents in the silver-clay antimicrobial agents were in the range of 1.9–4.4 wt%. The glazes were prepared from a base frit consisting of 69.5 SiO_2, 14.4 Al_2O_3, 9.9 CaO, 3.6 K_2O and 2.5 Na_2O (wt%) and glazed bodies were fired in both oxidising and reducing atmospheres. A suspension of *E. coli* was employed for evaluation of antimicrobial activity. The glazes with 10 wt% antimicrobial agents, fired at 1300 °C in a reducing atmosphere, showed negative antimicrobial activities. In these glazes, the loss of Ag after reduction firing is evident, likely due to the reactivity of Ag with a reducing gas containing CO. On the other hand, the antimicrobial activities of the glazes with 10 wt% of the agents fired in an oxidising atmosphere were encouraging. The glaze with an agent doped with Zr exhibited a high antimicrobial activity upon adding only 0.2 wt% of the agent, resulting in only 0.008 wt% Ag in the glaze.

Glazes showing aesthetic superficial effects

As has been mentioned, glass–ceramic glazes were initially developed with the aim of enhancing the technological properties of the surface of glazed ceramic tiles, such as hardness, scratch or resistance. Nevertheless, in addition to the functional aspects, the glaze is also responsible for the aesthetic aspect of the ceramic tile. Aesthetic concerns include a variety of surface finishes, including degrees of gloss and matte, colour and special surface appearances, such as the aventurine effect of metallic lustre.

The aventurine effect

'Aventurine glaze' is the generic name for glazes containing macroscopic laminar crystals, which cause a decorative effect of sparkling, i.e. deeper lustre caused by light rays falling on the glaze surface, which resembles the effect of the natural mineral aventurine [163]). In these glazes, the sparkling effect is due to the difference in the light-reflection coefficients between the crystalline and glassy phases and depends on the size, shape, quantity and arrangement of crystals and on the observation angle [164, 165].

The elements able to crystallise as metals or oxides and give rise to the aventurine effect are Fe, Cr, Cu, Ni, Mn and U. The optimum concentration of the metal oxide varies for each type of composition. If low, it dissolves into the glass and does not produce the effect, while if too high can result in large crystals on the surface and give a metallic appearance, instead of the aventurine effect [166]. The copper aventurines result from the crystallisation of Cu^0 [167]; in chrome aventurine, hexagonal crystals of fuchsita (Cr_2O_3) develop [168]; whereas in iron aventurine the crystallisation of hematite (Fe_2O_3) [169, 170] or mixtures of hematite and fayalite (Fe_2SiO_4) [171] are observed.

Without doubt, Fe_2O_3 is the most reported oxide in the literature as effective generator of aventurine glazes. Levitskii [163], in a study to determine the conditions for obtaining aventurine effects in glaze coatings based on synthesised glasses, pointed out that the use of glass–iron oxide mixtures as the basis for aventurine glaze is more efficient than iron-bearing glasses, which have a lower crystallisation ability. For this reason, in most cases, Fe_2O_3 is mixed with a frit to result in the glaze. Since the laminar crystal growth requires a low viscosity melted phase, lead and boric frits with low alumina content are normally used. In general, Fe_2O_3 content in aventurine glazes is between 10 and 30 wt% and the effect depends on how this is introduced, whether as hematites or magnetite, and, particularly, on the composition of the base frit [166]. Thus, Romero et al. [113] showed that the distribution of Fe^{3+} ions among several crystalline phases in glazes developed from mixtures of Zn- and Fe-containing frits, depends on the iron content in the frit. Accordingly, in these glazes an iron content lower than 9 wt% leads to glass–ceramic glazes with all Fe^{3+} ions crystallised as franklinite

($ZnFe_2O_4$). Iron content close to 15 wt% gives rise to franklinite as the main crystalline phase but Fe^{3+} ions begin to crystallise as hematite. When iron content approaches 19 wt% a change in the relative proportions of the crystalline phases occurs, and hematite becomes the main crystalline phase crystallised in the glaze. An iron content greater than 22 wt% leads to a glass–ceramic glazes with all Fe^{3+} ions crystallised as hematite.

The mechanism involved in producing the aventurine effect in glazes with iron oxides entails two steps: dissolution in the melt and subsequent hematite crystallisation at lower temperature.

However, in spite of the substantial literature regarding aventurine glazes, the difficulty obtaining aventurine effect at industrial level, together with the clear dependence on the glaze composition and above all, on the firing cycle, have relegated the application of aventurine effects to artistic ceramics, preventing its application in the industrial manufacture of ceramic tiles with firing curves not longer than 60 min. Fortunately, Casañ et al. [172] in a recent paper have reported on the aventurine effect in ceramic glazed tiles with shorter firing schedules than those recommended by the literature, which can be easily adapted to standardised industrial production.

Metallic lustrer

Having begun long ago, the production of ceramic pieces with metallic finish and with a golden, silver or chrome plated aspect has not stopped, using these effects in the development of friezes, profiles, special pieces and small format wall tiles [173]. Traditionally, the production of such effects was achieved by the technique of the third fire, which involves the application of a solution of noble metals (gold, silver and platinum) on a fired tile, followed of a new low-temperature firing. This process involves high cost in both raw materials and production. In addition, most formulas used to obtain a metallic effect contain sulphur and organic substances that in many cases include mercury. Moreover, all silver compounds are toxic. For this reason, in recent years different research groups have focused their investigations on the development of glass–ceramic glazes with similar effects to those produced by precious metals in terms of gloss, lustre and colour.

Thus, Cabrera et al. [173] reported the development by a fast-firing process of glass–ceramic glazes composed mainly of 24–51 SiO_2, 7–21 Al_2O_3, 10–30 Fe_2O_3 and 7–27 P_2O_5 (wt%), which reproduce the appearance of metals. In the formulations of these glazes, precious metals or additional firing steps have not been used. The metallic effect is due to the crystallisation of an iron phosphate phase with modified structure, which is formed on the surface of the glaze, with a very pronounced preferred orientation. This crystalline phase is developed during cooling and it appears to grow from a liquid phase separation.

In two recent papers, Siligardi et al. [174] have studied the formation of the lustre effect in glazes manufactured from copper- and ceria-containing frits [175]. Glazes developed from a frit composed of 68 SiO_2, 3 Al_2O_3, 12 CuO, 5 Na_2O, 2 ZnO and 10 CaO (mol%) present a reddish and light bluish reflective metallic surface due to the crystallisation of dendritic tenorite (CuO) at the surface of the glaze. The authors deduced that the Cu(I) contained in the glass underwent a dismutation reaction, giving rise to the presence of Cu(II), which, in presence of oxygen, led to the formation of tenorite (CuO) and to Cu metal segregation in the very outmost surface because of the peculiar brilliancy of the glazes. As for the metallic effect developed by Ce-containing glazes, the authors have pointed out that a cerium oxide content lower than 1 mol% does not show any particular aesthetic effect because no surface ceria crystallisation occurred, while glazes containing 3 and 6 mol% of CeO_2 show lustre surface due to ceria crystallisation. A detailed study of a glaze developed from a frit containing 47.7 SiO_2, 9.6 ZnO, 7.2 Al_2O_3, 7.8 CaO, 6.3 B_2O_3 and 8.7 CeO_2 (wt%), and other minor oxides such as BaO, ZrO_2, Na_2O, K_2O and MgO has shown that the glazed tile surface presents a reflective lustre and an iridescent surface due to the crystallisation of a very thin crystalline layer of ceria (CeO_2) at the surface of the glaze. In this case, ceria crystallisation occurs at about 900 °C during the heating cycle and no relevant transformation occurs during the cooling step.

Conclusions

This review provides an overview of the different systems that have led to the development of glass–ceramic glazes with improved mechanical and chemical properties compared to traditional ceramic glazes. Increased quality of life requires new building materials with environment improving characteristics and thus, it became essential to develop new glazes with specific properties to comply with the requirements of both society and the ceramic tile industry. These demands can only be achieved through proper design of glass–ceramic compositions, which will lead to the achievement of favourable properties (thermal, optical, chemical, mechanical and biological) through the development of an appropriate microstructure. However, not all glass compositions are suitable for appropriate glass–ceramic glazes and several criteria (viscosity on firing, expansion coefficient and surface tension) govern the design of parent frits. Moreover, it is necessary to control the crystallisation process to obtain a product with appropriate technical properties and adequate aesthetics. Finally, it is necessary to remark that although many glass systems have been tested to develop glass–ceramic glazes, there are still many frit compositions to be explored, through which improved properties (e.g. heat absorption, fluorescence and insulation) could be achieved.

Acknowledgements The authors want to thank Mr. R. Rincón for the kind assignment of the Ishtar gate photograph shown in Fig. 4 and to Ms. D. Fernández and Mr. E. Fernández (Department of Library and Publications, IETcc-CSIC) for their assistance in compiling the references necessary for the completion of this review. R. Casasola is grateful to the Spanish National Research Council (CSIC) for her contract through the JAE Program (JAE Pre_08_00456). Financial support through the project MAT2006-05977 (Education and Science Spanish Ministry) is also recognised.

References

1. Willhauk E, Harikantha R (2005) In: Bach H, Krause D (eds) Low thermal expansion glass-ceramics, 2nd edn. Springer Verlag, Heidelberg, p 51. doi:10.1007/3-540-28245-9_3
2. Rawlings RD, Wu JP, Boccaccini AR (2006) J Mater Sci 41:733. doi:10.1007/s10853-006-6554-3
3. Michie EM, Grimes RW, Boccaccini AR (2008) J Mater Sci 43:4152. doi:10.1007/s10853-007-2232-3
4. Romero M, Kovacova M, Rincón JM (2008) J Mater Sci 43:4135. doi:10.1007/s10853-007-2318-y
5. Kanchanarat N, Bandyopadhyay-Ghosh S, Reaney IM, Brook IM, Hatton PV (2008) J Mater Sci 43:759. doi:10.1007/s10853-007-2180-y
6. Griggs JA, Anusavice KJ, Mlecholsky JJ (2002) J Mater Sci 37:2017. doi:10.1023/A:1015255300065
7. Bretcanu O, Spriano S, Brovarone Vitale C, Verné E (2006) J Mater Sci 41:1029. doi:10.1007/s10853-005-2636-x
8. Romero M, Rincón JM (1996) Mater Constr 46:91. doi:103989/mc1996v46i242-243532
9. Arnault L, Gerland M, Rivière A (2000) J Mater Sci 35:2331. doi:10.1023/A:1004716018522
10. Prewo KM (1986) J Mater Sci 21:3590. doi:10.1007/BF00553805
11. Chaim R, Muñoz A, Miranda H, Dominguez-Rodriguez A (1996) J Mater Sci 31:3887. doi:10.1007/BF00352806
12. Vaidya RU, Subramanian KN (1991) J Mater Sci 23:6453. doi:10.1007/BF00551896
13. Rincón JM (1992) Polym Plast Technol Eng 31:309. doi:10.1080/03602559208017751
14. Tamman G (1903) Kristallisieren und Schmelzen. Johann Ambrosius Barth, Leipzig
15. McMillan PW (1979) Glass–ceramics, 2nd edn. Academic Press Inc, London
16. Strnad Z (1986) Glass–ceramic materials. Elsevier, Amsterdam
17. Manfredini T, Pellacani GC, Rincón JMa (1997) Glass–ceramic materials, fundamentals and applications. Mucchi Editore, Modena
18. Hölland W, Beall G (2002) Glass–ceramic technology. The American Ceramic Society, Westerville
19. Gregory AG, Veasey TJ (1971) J Mater Sci 6:1312. doi:10.1007/BF00552045
20. Morrell R, Ashbee KHG (1973) J Mater Sci 8:1253. doi:10.1007/BF00549340
21. Partridge G (1994) Glass Technol 35:116
22. Vicente-Mingarro I, Callejas P, Rincón JMa (1993) Bol Soc Esp Ceram V 32:157
23. James PF (1995) J Non-Cryst Solids 181:1. doi:10.1016/0022-3093(94)00515-X
24. Pannhorst W (1997) J Non-Cryst Solids 219:198. doi:10.1016/S0022-3093(97)00270-6
25. Rasteiro MG, Gassman T, Santos R, Antunes E (2007) Ceram Int 33:345. doi:10.1016/j.ceramint.2005.10.002
26. Lo CL, Duh JG, Chiou BS (2003) J Mater Sci 38:693. doi:10.1023/A:1021836326089
27. Chen GH (2007) J Mater Sci 42:7239. doi:10.1007/s10853-007-1548-3
28. Richerson DW (2000) The magic of ceramics. The American Ceramic Society, Westerville
29. www.spaintiles.info. Accessed 20 June 2011
30. Quinteiro E, Ortega A, Leonelli C, Manfredini T, Siligardi C (2003) Ceram Inf 302:62
31. Parmelee C, Harman C (1973) Ceramic glazes, 3rd edn. CBLS, Marietta
32. Matthes WE (1995) Vidriados cerámicos. Omega, Barcelona
33. Graham J (1975) Am Miner 60:919
34. Wang D, Guo Y, Liang K, Tao K (1999) Sci China Ser A 42:80. doi:10.1007/BF02872053
35. French RH, Glass SJ, Ohuchi FS, Xu YN, Ching WY (1994) Phys Rev B 49:5133
36. Anseau MR, Di Rupo E, Cambier F (1981) J Mater Sci 16:825. doi:10.1007/BF02402802
37. www.iuvenisorbis.org/mineralogy
38. Merlini M, Gemmi M, Artioli G (2005) Phys Chem Miner 32:189. doi:10.1007/s00269-005-0458-7
39. Deganello S (1973) Z Kristallogr 137:127. doi:10.1524/zkri.1973.137.2-3.127
40. Siegesmund S, Mosch S, Scheffzük CH, Nikolayev DI (2008) Environ Geol 55:1437. doi:10.1007/s00254-007-1094-y
41. Wiff JP, Kinemuchi Y, Naito S, Uozumi A, Watari K (2009) J Mater Res 24:1989. doi:10.1557/jmr.2009.0241
42. PDF MaintEx library (version 9.0.133) from EVA 13, 0, 0, 3 Copyright © Bruker-AXS 1996-2007 program
43. http://www.diffen.com/difference/cubic_zirconia_vs_diamond. Accessed 20 June 2011
44. Smyth JR, Jacobsen SD, Hazen RM (2000) In: Hazen RM, Downs RT (eds) High-temperature and high pressure crystal chemistry. Mineralogical Society of America, Arizona, p 157
45. Gallé C, Sercombe J (2001) Mater Struct 34:619. doi:10.1007/BF02482129
46. Bartha P (1989) In: Zhong X (ed) Proceedings of international symposium on refractories–refractory raw materials and high performance refractory products, Hangzhou
47. Pérez-Centeno A, López-Contreras OE, Rubio-Avalos JC, Alonso-Guzmán EM, Martínez-Molina W, Manzano-Ramírez A, Pérez-Tijerina E, Avalos-Borja M (2006) In: 8th Microscopy National Congress, Acapulco. http://www.amemi.org/congreso/MATERIALES/MP5.pdf
48. Bhatkar VB, Bhatkar NV (2011) Int J Adv Eng Sci Technol 5:184. http://www.ijaest.iserp.org
49. Cong Y, Li B, Yue S, Fan S, Wang XJ (2009) J Phys Chem C 113:13974. doi:10.1021/jp8103497
50. Liang J, Deng Z, Jiang X, Li F, Li Y (2002) Inorg Chem 41:3602. doi:10.1021/ic025532q
51. Meinssen K (1997) Ceram Eng Sci Proc 18:308. doi:10.1002/9780470294420.ch30
52. Blonski R (1994) Ceram Eng Sci Proc 15:249. doi:10.1002/9780470314340.ch28
53. Escardino A, Moreno A, Amoros JL, Gozalbo A, Aparici J, Sanchez L (1996) In: Proceedings of IV world congress on ceramic tile quality, Castellon
54. Escardino A (2001) J Am Ceram Soc 84:23. doi:10.1111/j.1151-2916.2001.tb00602.x

55. Romero M, Rincón JM, Acosta A (2003) J Eur Ceramic Soc 23:1629. doi:10.1016/S0955-2219(02)00415-6
56. Jacobs CWF (1954) J Am Ceram Soc 37:216. doi:10.1111/j.1151-2916.1954.tb14026.x
57. Taylor JR, Bull AC (1986) Ceramics glaze technology. Pergamon Press, Oxford
58. Levitskii IA (2003) Glass Ceram 60:83. doi:10.1023/A:1024779814735
59. Sehlke KH, Tauber A (1969) Trans Br Ceram Soc 68:53
60. El-Defrawi SA, Serry MA, Abd El-Fattah WI, Weisweiler W (1995) Ceram Int 21:69. doi:10.1016/0272-8842(95)95874-H
61. Aparici J, Moreno A, Escardino A, Amorós JL, Mestre S (1994) In: Proceedings of II world congress on ceramic tile quality, Castellon
62. Castilone RJ, Sriram D, Carty WM, Snyder RL (1999) J Am Ceram Soc 82:2819. doi:10.1111/j.1151-2916.1999.tb02162.x
63. Amoros JL, Escardino A, Orts MJ, Moreno A (1994) Br Ceram Trans 93:224
64. Ssifaoui A, Atmani W, Daoudi A, Moussa R, Blanchart P (2003) Br Ceram Trans 102:57. doi:10.1179/096797803225001650
65. Bobkova NM, Levitskii IA, Gailevich SA, Kolontaeva TV (1999) Glass Ceram 56:22. doi:10.1007/BF02681398
66. Karasu B, Dölekçekiç E, Özdemir B (2001) Br Ceram Trans 100:81. doi:10.1179/096797801681251
67. Vicent JB, Ros JL, Tena MA, Escribano P, Monros G (1998) In: Proceedings of V world congress on ceramic tile quality, Castellon
68. Ruiz O, Sanmiguel F, Rubio J, Oteo JL, Sánchez-Cortés S (2007) Ceram Inf 337:130
69. Monrós G, et al. (1998) In: Proceedings of V world congress on ceramic tile quality, Castellon
70. Generali E, Baldi G, Ferrari AM, Leonelli C, Manfredini T, Siligardi C, Pellacani GC (1995) Ceram Inf 358:16
71. Llusar M, Rodrigues C, Labrincha J, Flores M, Monrós G (2002) J Eur Ceram Soc 22:639. doi:10.1016/S0955-2219(01)00339-9
72. Schabbach LM, Bondioli F, Ferrari AM, Manfredini T, Petter CO, Fredel MC (2007) J Eur Ceram Soc 27:179. doi:10.1016/j.jeurceramsoc.2006.04.180
73. Wycoff R (1965) Crystal structures, 3rd edn. Wiley, New York
74. Earl DA, Clark DE (2000) J Am Ceram Soc 83:2170. doi:10.1111/j.1151-2916.2000.tb01531
75. Concepcion C, Oteo J, Ocaña E, Rubio J, Velasco M (1997) Ceram Eng Sci Proc 18:96. doi:10.1002/9780470294420.ch11
76. Sorlí S, Tena MA, Mestre A, Llusar M, Monrós G (2004) In: Proceedings of VIII world congress on ceramic tile quality, Castellon
77. Rudkovskaya NV, Mikhailenko NY (2001) Glass Ceram 58:387. doi:10.1023/A:1014958309094
78. Karasu B, Çaki M, Turan S (2000) J Eur Ceram Soc 20:2225. doi:10.1016/S0955-2219(00)00075-3
79. Karasu B, Çaki M, Yeşilbaş YG (2001) J Eur Ceram Soc 21:1131. doi:10.1016/S0955-2219(00)00296-X
80. Xiaozhong Z, Guying Z (1985) Bull Chin Silic Soc 4:10
81. Xiaozhong Z (1993) J Chin Ceram Soc 21:38
82. Norton FH (1937) J Am Ceram Soc 20:217. doi:10.1111/j.1151-2916.1937.tb19892.x
83. Takashima H (1982) Ceram Int 8:74. doi:10.1016/0272-8842(82)90019-0
84. Karasu B, Turan S (2002) J Eur Ceram Soc 22:1447. doi:10.1016/S0955-2219(01)00456-3
85. Sun C, Kuan C, Kao FJ, Wang YM, Chen JC, Chang CC, Shen P (2004) Mat Sci Eng A 379:327. doi:10.1016/j.msea.2004.02.063
86. Eftekhari Yekta B, Alizadeh P, Rezazadeh L (2007) J Eur Ceram Soc 27:2311. doi:10.1016/j.jeurceramsoc.2006.08.009
87. Bou E, García-Ten J, Pérez R, Arrufat S, Atichian G (2010) Bol Soc Esp Ceram V 49:271
88. Torres FJ, Ruiz de Sola E, Alarcón J (2005) J Non-Cryst Solids 351:2453. doi:10.1016/j.jnoncrysol.2005.06.027
89. Torres FJ, Ruiz de Sola E, Alarcón J (2006) J Eur Ceram Soc 26:2285. doi:10.1016/j.jeurceramsoc.2005.04.020
90. Torres FJ, Ruiz de Sola E, Alarcón J (2006) J Non-Cryst Solids 352:2159. doi:10.1016/j.jnoncrysol.2006.01.038
91. MacDowell JF, Beall GH (1969) J Am Ceram Soc 52:17. doi:10.1111/j.1151-2916.1969.tb12653.x
92. Yuritsin N, Fokin V, Kalinina A, Filipovich V (1992) Bol Soc Esp Ceram V 31-C:21
93. Mueller R, Thamm D, Pannhorst W (1992) Bol Soc Esp Ceram V 314:105
94. De Vekey RC, Majumdar AJ (1975) Phys Chem Glas 16:36
95. Wu JM, Hwang SP (2001) J Am Ceram Soc 84:1108. doi:10.1111/j.1151-2916.2001.tb00797.x
96. Sung YM (1996) J Mater Sci 31:5421. doi:10.1007/BF01159312
97. Beall H, Doman RC (1980) Sci Ceram 10:25
98. Ferrari AM, Barbieri L, Leonelli C, Manfredini T, Siligardi C, Corradi AB (1997) J Am Ceram Soc 80:1757. doi:10.1111/j.1151-2916.1997.tb03049.x
99. De Vekey RC, Majumdar AJ (1974) Glass Technol 15:71
100. Vila J, Valentín C, Muñoz MC, Sales M, Alarcón J (1998) Bol Soc Esp Ceram V 38:390
101. Sales M, Alarcón J (1995) J Mater Sci 30:2341. doi:10.1007/BF01184584
102. Torres FJ, Alarcón J (2003) J Eur Ceram Soc 23:817. doi:10.1016/S0955-2219(02)00206-6
103. Watanabe K, Giess EA, Shafer MW (1985) J Mater Sci 1985:508. doi:10.1007/BF01026520
104. Torres FJ, Alarcón J (2004) J Am Ceram Soc 87:1227. doi:10.1111/j.1151-2916.2004.tb07717.x
105. Torres FJ, Alarcón J (2005) Ceram Int 31:683. doi:10.1016/j.ceramint.2004.07.009
106. Martínez J, Marinova I, Rincón RJ, Valencia JS, Peiró M, Núñez I, Navarro E, Carda JB (2007) Ceram Inf 346:73
107. Rincón RJ, Benet MP, Juárez J, Cabezón C, Pedra JM, Carda JB, Martínez J (2009) Ceram Inf 367:49
108. Torres FJ, Alarcón J (2005) J Eur Ceram Soc 25:349. doi:10.1016/j.jeurceramsoc.2004.01.025
109. Atkinson DIH, McMillan PW (1976) J Mater Sci 11:994. doi:10.1007/BF00553107
110. Kim HS, Rawling RD, Rogers PS (1989) J Mater Sci 24:1025. doi:10.1007/BF01148794
111. Carter S, Ponton CB, Rawling RD, Rogers PS (1988) J Mater Sci 23:2622. doi:10.1007/BF01111924
112. Baldi G, Generali E, Leonelli C, Manfredini T, Pellacani GC, Siligardi C (1995) J Mater Sci 30:3251. doi:10.1007/BF01209246
113. Romero M, Rincón JM, Acosta A (2002) J Eur Ceram Soc 22:883. doi:10.1016/S0955-2219(01)00395-8
114. Torres FJ, Alarcón J (2004) J Non-Cryst Solids 347:45. doi:10.1016/j.jnoncrysol.2004.09.003
115. Yekta BE, Alizadeh P, Rezazadeh L (2006) J Eur Ceram Soc 26:3809. doi:10.1016/j.jeurceramsoc.2005.12.016
116. Pekkan K, Karasu B (2009) J Eur Ceram Soc 29:1571. doi:10.1016/j.jeurceramsoc.2008.10.010
117. Fröberg L, Kronberg T, Hupa L, Hupa M (2007) J Eur Ceram Soc 27:1671. doi:10.1016/j.jeurceramsoc.2006.05.012
118. Fröberg L, Hupa L, Hupa M (2009) J Eur Ceram Soc 29:7. doi:10.1016/j.jeurceramsoc.2008.04.037
119. Fröberg L, Kronberg T, Hupa L (2009) J Eur Ceram Soc 29:2153. doi:10.1016/j.jeurceramsoc.2009.01.012
120. Reinosa JJ, Rubio-Marcos F, Solera E, Bengochea MA, Fernández JF (2010) Ceram Int 36:1845. doi:10.1016/j.ceramint.2010.03.029

121. Sanmiguel F, Ferrando V, Mestre A, Monros G (2000) In: Proceedings of VI world congress on ceramic tile quality, Castellon
122. Benet MPS, Pianaro SA, Piquer S, Peiró MC, Núñez I, Navarro E, Carda JB (2006) Ceram Inf 332:37
123. Escardino A, Amorós JL, Gozalbo A, Orts MJ, Lucas F, Belda A (2002) In: Proceedings of VII world congress on ceramic tile quality, Castellon
124. Kronberg T, Hupa L, Fröberg K (2004) Key Eng Mater 264–268:1565
125. Vane-Tempest S, Kronberg T, Fröberg L, Hupa L (2004) In: Proceedings of VIII world congress on ceramic tile quality, Castellón
126. Hupa L, Bergman R, Fröberg L, Vane-Tempest S, Hupa M, Kronberg T, Pesonen-Leinonen E, Sjöberg AM (2005) Surf Sci 584:113
127. Fröberg L, Kronberg T, Törnblom S, Hupaa L (2007) J Eur Ceram Soc 27:1811. doi:10.1016/j.jeurceramsoc.2006.04.162
128. JMa Rincón, Romero M, Marco J, Caballer V (1998) Mater Res Bull 33:1159. doi:10.1016/S0025-5408(98)00109-3
129. Leonelli C, Manfredini T, Paganelli M, Pellacani GC, Amorós JL, Enrique JE, Orts MJ, Bruni S, Cariati F (1991) J Am Ceram Soc 74:983. doi:10.1111/j.1151-2916.1991.tb04331.x
130. Romero M, Rincón JMa, Acosta A (2004) J Am Ceram Soc 87:819. doi:10.1111/j.1551-2916.2004.00819.x
131. Escribano P, Carda JB, Cordoncillo E (2001) Esmaltes y pigmentos cerámicos. Faenza Editrice Ibérica, Castellón
132. Fortanet E, Gabaldón S, Bakali J, Núñez I, Peiró M, Carda JB (2007) Ceram Inf 338:72
133. Campa F, Ginés F, Robles J (2000) In: Proceedings of VI world congress on ceramic tile quality, Castellon
134. Quinteiro E, Carvalho JC, Menegazzo BA, Manegazzo APM, Silva VA, Silva NG (2004) In: Proceedings of VIII world congress on ceramic tile quality, Castellon
135. Tomizaki MF, Shinkai S (1995) J Ceram Soc Jpn 103:330
136. Toya T, Tamura Y, Kameshima Y, Okada K (2004) Ceram Int 30:983. doi:10.1016/j.ceramint.2003.11.005
137. Toya T, Nakamura A, Kameshima Y, Nakajima A, Okada K (2007) Ceram Int 33:573. doi:10.1016/j.ceramint.2005.11.009
138. Cheng TW (2004) Chemosphere 56:127. doi:10.1016/j.chemosphere.2004.02.009
139. Matteucci F, Cruciani G, Dondi M, Guarini G, Raimondo M (2004) In: Proceedings of VIII world congress on ceramic tile quality, Castellon
140. Kuchinski FA (1993) In: Wachtman JB, Haber RK (eds) Ceramic films and coatings. Noyes Publications, New Jersey, p 77
141. Eppler RA (1971) J Am Ceram Soc 54:595. doi:10.1111/j.1151-2916.1971.tb16012.x
142. Eppler RA, McLeran WA Jr (1967) J Am Ceram Soc 50:152. doi:10.1111/j.1151-2916.1967.tb15067.x
143. Biffi G, Ortelli G, Vincenzini P (1975) Ceram Int 1:34
144. Moreno A, Bou E, Mestre S, Navarro MC (1998) In: Proceedings of V world congress on ceramic tile quality, Castellon
145. Teixeira S, Bernardin AM (2009) Dyes Pigments 80:292. doi:10.1016/j.dyepig.2008.07.017
146. Escardino A, Moreno A, Bou E, Ibáñez MJ, Muñoz A, Barba A (2004) In: XLIV annual congress of the spanish ceramic and glass society, Vigo
147. Bou E, Moreno A, Escardino A, Gozalbo A (2007) J Eur Ceram Soc 27:1791. doi:10.1016/j.jeurceramsoc.2006.04.148
148. Chen SK, Liu HS (1994) J Mater Sci 29:2921. doi:10.1007/BF01117602
149. Rodriguesa J, Bernardin AM (2010) In: Proceedings of XI world congress on ceramic tile quality, Castellon
150. Atkinson I, Teoreanu I, Mocioiu OC, Smith ME, Zaharescu M (2010) J Non-Cryst Solids 356:2437. doi:10.1016/j.jnoncrysol.2010.04.054
151. Pinckney LR, Beall GH (1997) J Non-Cryst Solids 219:219. doi:10.1016/S0022-3093(97)00272-X
152. Beall GH, Pinckney LR (1999) J Am Ceram Soc 82:5. doi:10.1111/j.1151-2916.1999.tb01716.x
153. Glaze W, Kang JW, Chapin DH (1987) Sci Eng 9:335
154. Munter R (2001) Proc Est Acad Sci Chem 50:59
155. Fujishima A, Rao TN, Tryk DA (2000) J Photochem Photobiol C 1:1. doi:10.1016/S1389-5567(00)00002-2
156. Han F, Kambala VSR, Srinivasan M, Rajarathnam D, Naidu R (2009) Appl Catal A 359:25. doi:10.1016/j.apcata.2009.02.043
157. Stasinakis AS (2008) Global NEST J 10:376
158. Meseguer S, Galindo F, Sorlí S, Cargori C, Tena MA, Monrós G (2006) Ceram Inf 333:61
159. Ruiz O, Sanmiguel F, Gargori C, Galindo F, Monrós G (2008) In: Proceedings of X world congress on ceramic tile quality, Castellon
160. Zeng Z, Peng C, Hong Y, Lu Y, Wu J (2010) J Am Ceram Soc 93:2948. doi:10.1111/j.1551-2916.2010.03910.x
161. Qing X, Wen C, Feng Z, Run-Zhang Y (2002) J Wuham Univ Technol 17:11
162. Yoshida H, Abe H, Taguri T, Ohashi F, Fujino S, Kajiwara T (2010) J Ceram Soc Jpn 118:571
163. Levitskii IA (2001) Glass Ceram 58:223. doi:10.1023/A:1012351301045
164. Callejas P, MaF Barba, JMa Rincón (1985) J Mater Sci Lett 4:1171. doi:10.1007/BF00720446
165. Rincón JMa, Callejas P (1988) J Mater Sci 23:1042. doi:10.1007/BF01154009
166. Gozalbo A, Orts MJ, Mestre S, Gómez P, Agut P, Lucas F, Belda A, Blanco C (2006) In: Proceedings of IX world congress on ceramic tile quality, Castellon
167. Shcheglova MD, Babenko TV, Polozhai SG, Svistun VM (1996) Glass Ceram 53:14. doi:10.1007/BF01171391
168. Takahashi S, Nishimura Y, Tabata H, Shimizu T (2001) Jpn J Appl Phys 40:L961. doi:10.1143/JJAP.40.L961
169. Dvornichenko IN, Matsenko SV (2000) Glass Ceram 57:67. doi:10.1007/BF02681489
170. Gozalbo A, Orts MJ, Mestre S, Gómez P, Agut P, Lucas F, Belda A, Blanco C (2007) Ceram Inf 339:80
171. Pearson RS, Pearson BI (1992) Ceram Porton Artes 44:52
172. Casañ E, Lleo E, Palomares F, Rodriguez V, Martí V, Seores J, Cabrera MJ (2010) Bol Soc Esp Ceram V 49:142
173. Cabrera MJ, Montins V, Foó A, Balfagón P (2007) Ceram Inf 332:63
174. Siligardi C, Montecchi M, Montorsi M, Pasqualiz L (2009) J Am Ceram Soc 92:2784. doi:10.1111/j.1551-2916.2009.03250.x
175. Siligardi C, Montecchi M, Montorsi M, Pasqualiz L (2010) J Am Ceram Soc 93:2545. doi:10.1111/j.1551-2916.2010.03880.x